*Dynamics of an expanding black rhinoceros (*Diceros bicornis minor*) population*

Peter R. Law, Brad Fike & Peter C. Lent

European Journal of Wildlife Research

ISSN 1612-4642
Volume 61
Number 4

Eur J Wildl Res (2015) 61:601-609
DOI 10.1007/s10344-015-0935-3

Springer

Eur J Wildl Res (2015) 61:601–609
DOI 10.1007/s10344-015-0935-3

ORIGINAL PAPER

Dynamics of an expanding black rhinoceros (*Diceros bicornis minor*) population

Peter R. Law[1] · **Brad Fike**[2] · **Peter C. Lent**[3]

Received: 15 August 2014 / Revised: 20 May 2015 / Accepted: 26 May 2015 / Published online: 6 June 2015

Abstract Understanding population dynamics is critical for meta-population management, especially of endangered species, and also for megaherbivore ecology. We employed complete individual life records to construct census data for a reintroduced black rhinoceros population over 22 years since its founding and investigated its dynamics. Akaike's information criterion applied to scalar models of population growth based on the generalized logistic unambiguously selected an exponential growth model (r=0.102±0.017), indicating a highly successful reintroduction. No evidence of density dependence was detected, and thus, we could not confirm the threshold model of density dependence that has influenced black rhinoceros meta-population management. Our analysis supported previous work contending that the generalized logistic is unreliable when fitted to data that do not sample the entire range of population sizes. A stage-based matrix model of the exponential population dynamics exhibited mild transient behaviour. We found no evidence of environmental stochasticity, consistent with our previous studies of this population that found no influence of rainfall on demographic parameters. Demographic stochasticity was present, principally reflected in annual sex-specific recruitment numbers that differed from deterministic predictions of the matrix model. Demographically driven process noise should be assumed to be a component of megaherbivore population dynamics, as these populations are typically relatively small, and should be accounted for in managed removals and introductions. Increase in age at first reproduction with increasing population size, as manifested in the study population, may provide a warning of possible density feedback prior to detectable slowing of population growth rate for megaherbivores.

Keywords Black rhinoceros · Density dependence · Megaherbivores · Population dynamics · Transient dynamics · Stochasticity

Communicated by H. Kierdorf

Electronic supplementary material The online version of this article (doi:10.1007/s10344-015-0935-3) contains supplementary material, which is available to authorized users.

✉ Peter R. Law
prldb@member.ams.org

[1] Centre for African Conservation Ecology, Nelson Mandela Metropolitan University, P.O. Box 77000, Port Elizabeth 6031, Republic of South Africa

[2] P.O. Box 4038, Rosehill Mall, Port Alfred 6170, Republic of South Africa

[3] Department of Zoology and Entomology, University of Fort Hare, Alice 5700, Republic of South Africa

Introduction

Reintroduction is an important strategy of conservation science (Seddon et al. 2007) and a critical component of meta-population management for endangered rhinoceros species (Emslie 2001; Emslie et al. 2009). Since reintroductions are sourced from existing populations, understanding population dynamics is vital to conservation theory and practice as regards both the expected performance of the introduced population and possible effects on the donor population (Armstrong and Seddon 2007). Slowing rates of increase in potential source populations led Emslie et al. (2009) to stress the need for predictive models to aid meta-population management for all species of rhinoceros. Population dynamics are a vital component in this effort, which also embraces populations recovering from poaching (Brodie et al. 2011).

The approach to meta-population management for black rhinoceros (*Diceros bicornis*) of Emslie (2001) assumed a threshold model of density dependence (McCullough 1992, 1999) involving exponential growth from low abundance to near equilibrium followed by a rapid decline in population growth rate to zero (S3) (equations, etc., numbered with a prefix "S" refer to the Supplementary Online Resource). However, the scarcity of undisturbed expanding populations of rhinoceros and other megaherbivores poses an obstacle to testing that hypothesis of megaherbivore ecology. There are few long-term studies of megaherbivore population dynamics (Owen-Smith 2010), especially based on census data.

For not only rhinoceros ecology and conservation in particular but also megaherbivore ecology in general, components of dynamics requiring attention include density dependence (Bonenfant et al. 2009; Owen-Smith 2010), transient dynamics (Koons et al. 2005), and both environmental and demographic stochasticity (Lande et al. 2003; Engen et al. 2005; Owen-Smith 2010); see also Morris and Doak (2002). Even with census data, however, extracting ecological information faces challenges prescribing and fitting models to abundance data (Polansky et al. 2009; Clark et al. 2010).

Our dataset consisted of a time series of censuses of a black rhinoceros (*D. bicornis minor*) population that grew monotonically from its reintroduction in 1986 through the end of 2008 without reaching equilibrium. We fitted scalar models of population growth to these data to evaluate whether density dependence acted during this time and explored the difficulties mentioned above with fitting models. We estimated demographic and environmental stochasticity for the unstructured population using the best-fit scalar model (Lande et al. 2003; Morris and Doak 2002).

We next built a matrix model to assess the relevance of population structure to the dynamics, in particular, to check for transient dynamics (Koons et al. 2005) and to estimate demographic stochasticity for the structured population (Engen et al. 2005). That environmental variation can influence population dynamics is well known (Owen-Smith 2010). Demographic stochasticity may be important for reintroductions and perhaps for many populations of megaherbivores. Few estimates of demographic stochasticity have been reported for mammals.

This paper extends the study of a key population of the critically endangered black rhinoceros (Lent and Fike 2003; Ganqa et al. 2005; Ganqa and Scogings 2007; van Lieverloo et al. 2009; Fike 2011; Law et al. 2013, 2014) and contributes to the understanding of megaherbivore population dynamics (Cromsigt et al. 2002; Gough and Kerley 2006; Chamaillé-Jammes et al. 2008; Okita-Ouma et al. 2010; Owen-Smith 2010; Brodie et al. 2011; Lee et al. 2011; Okita-Ouma 2014) both for theoretical ecology and conservation science.

Methods

Study population and dataset

The Great Fish River Nature Reserve, Eastern Cape Province, South Africa, is split into halves by the Great Fish and Kat rivers and is considered an excellent black rhinoceros habitat. Black rhinoceros were independently introduced into each half of the reserve. The population in the 220-km^2 western sector (former Sam Knott and Kudu Reserve) is the older, larger, and more consistently monitored of the two and has been the focus of considerable study, as noted in the "Introduction." We refer to it from its founding in June 1986 through December 2008 as SKKR. SKKR was effectively isolated demographically and was monitored by ground patrols and aerial reconnaissance; each animal was ear-notched for identification, and all births and deaths were recorded. No animals were handled for the research reported in this paper.

A total of 23 individuals were successfully introduced, the final release in December 1997, five subadults were removed in May 2006, and the population grew monotonically on a semi-annual basis to reach 110 (26 calves, 39 subadults, and 45 adults) in December 2008. From complete population records, we computed population censuses each June and December, from June 1986 through December 2008 (Fig. 1). These census data excluded concerns of false signals of density dependence (Shenk et al. 1998; Freckleton et al. 2006; Bonenfant et al. 2009) or with conflating sampling error with process noise (deValpine and Hastings 2002). See the Online Resource and previously cited literature for further details of the population.

Scalar population models

Scalar models of density dependence are prominent in population studies of large herbivores (Owen-Smith 2010). Recognition that the linear decline in per capita growth rate of the logistic model is unrealistic for populations of large

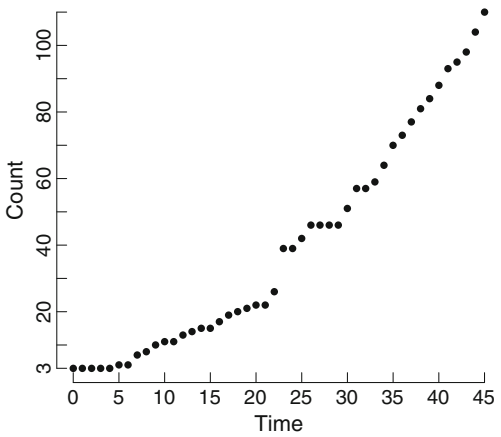

Fig. 1 Semi-annual census data, June 1986 to December 2008

vertebrates (Fowler 1981, 1987; McCullough 1992) favoured the generalized logistic as a flexible model of density dependence. Since black rhinoceros are aseasonal breeders, their population dynamics lack a natural time step. We write a continuous-time per capita growth equation and its solution in the form

$$\frac{N'}{N} = (\ln(N))' = f(N) \quad N(t) = F(t{-}s, N(s)) \tag{1}$$

$0 \le s < t$. For the generalized logistic,

$$f(N) = r\left[1-(N/K)^{\theta}\right], \tag{2}$$

(see S1 for F). Let N_t be the census data at time t. Non-linear regression fits these data to the solution by putting $\varepsilon_t = N_t - F(t, N_0)$, with ε_t independent $N(0,\sigma^2)$ variates. Since the projected value at t depends only on N_0 in this model, ε_t does not participate in the model dynamics and is not realistically modelled as process noise. We included this naïve model in our analyses to evaluate the importance of process noise.

Discrete-time models incorporate process noise in a straightforward fashion. A semi-annual time step should preclude a pronounced artificial time lag in discrete-time models of population dynamics for black rhinoceros. We considered three discretizations of Eq. (1) (Turchin 2003). One can replace N'/N by $(N_{t+1}-N_t)/N_t$; replace $(\ln(N))'$ by $\ln(N_{t+1})-\ln(N_t)=\ln(N_{t+1}/N_t)$; or use the solution of Eq. (1) to project the population at $t+1$ from the population at t. Applied to the continuous-time generalized logistic (Eq. (2)), we refer to the first discretization as the discrete generalized logistic (DGL), the second as the generalized Ricker (genRicker), and the third as the stepwise generalized logistic (SGL). The DGL figured prominently in Cromsigt et al. (2002) and Okita-Ouma et al. (2010) though the genRicker is considered more ecologically realistic. The SGL should be most faithful to continuous-time dynamics. Models of exponential growth can be obtained by taking the limit as K goes to infinity. Anticipating difficulty with obtaining estimates for θ (Nelder 1961), we fitted the continuous-time generalized logistic (CGL) and the SGL with θ as a parameter but also with fixed integer values 1–10, 15, 20, 30, 50, 60, 100, 120, and 190. The error structure can be modelled as additive (Cromsigt et al. 2002; Okita-Ouma et al. 2010), or as multiplicative (Polansky et al. 2009; Clark et al. 2010), on abundance, the latter additive on the logarithmic scale. The models that we compared are listed in Table 1.

All model projections were adjusted to reflect introductions and removals (pp. S5–S6). Non-linear regression (pp. S7–S9) was performed in Statistica 8 (Statsoft), the maximized likelihood of the data computed for each model, and Akaike information criterion (AIC_c) employed to compare models (Burnham and Anderson 2002). The two error structures, additive and multiplicative, involve different response variables, N_t and $X_t=\ln(N_t)$, respectively, and constitute separate analyses for AIC_c comparisons. However, the discrete-time exponential model with multiplicative error has the same likelihood for time series data as the likelihood model of Dennis et al. (1991) for the response X_t, which Dennis et al. (1991) recast as a likelihood model for the response N_t, using the log-normal distribution. This recast model can be compared using AIC_c with the models with additive error structure as these models have response variable N_t. Since the recast likelihood is equivalent to the likelihood of the discrete-time exponential model with multiplicative error, it provides a common reference for the two separate AIC_c analyses. To assess the influence of time step between censuses, we repeated the above analyses employing just the December census data.

The discrete-time exponential growth model with multiplicative error was unambiguously the best fit to the semi-annual census data and provided an estimate of the expected annual growth rate in the form e^r. For each December census, we tabulated the contribution that each individual of the census made through its own survival and recruitment of offspring at the next December census. The variance of these data yields a quantity $V_d(N_t)$ for each December. For each December, we put

$$\left[\frac{N_{t+1}}{N_t} - e^r\right]^2 = \sigma_e^2(N_t) + \frac{V_d(N_t)}{N_t} \tag{3}$$

where N_t is the population size for the December census in question and N_{t+1} that for the following December. Equation (3) is then solved for $\sigma_e^2(N_t)$. Weighted means of the quantities $V_d(N_t)$ and $\sigma_e^2(N_t)$ provide estimates of demographic and environmental stochasticity, respectively, for the unstructured population (Sæther et al. 1998a; Lande et al. 2003; Morris and Doak 2002; pp. S15–S16).

Matrix model

Since the semi-annual census data were best modelled by the discrete-time exponential, we constructed a stage-based, two-sex, birth-flow matrix model with semi-annual time step using the entire population history from June 1986 to December 2008. The biological states of interest were calf (dependent upon the mother, specifically, in association with its mother, less than 4 years old, and no younger calf present), subadult (no longer a calf but not yet an adult), and adult (for females, have given birth or at least 7 years old; for males, 8 or more years old) (Law et al. 2013; Law and Linklater 2014). Lacking paternity data, reproduction was assigned exclusively to females (Goodman 1969). We constructed two distinct parametrizations of the matrix model to assess robustness of results: MM1, adapted from the parametrization in Brault and Caswell (1993), and MM2, based on Caswell (2001, Section 6.1.1)

Table 1 Scalar models of population dynamics with two error structures

Model	Additive error	Multiplicative error
Continuous-time exponential (Cexp)	$N_t=N_0e^{rt}+\varepsilon_t$	$X_t=X_0+rt+\varepsilon_t$
Continuous-time generalized logistic (CGL)	$N_t=F(t,N_0)+\varepsilon_t$	$X_t=\ln(F(t,N_0))+\varepsilon_t$
Discrete-time exponential (Dexp)	$N_{t+1}=e^rN_t+\varepsilon_t$	$X_{t+1}=r+X_t+\varepsilon_t$
Discrete generalized logistic (DGL)	$N_{t+1}=N_t(1+f(N_t))+\varepsilon_t$	$X_{t+1}=X_t+\ln(1+f(N_t))+\varepsilon_t$
Generalized Ricker (genRicker)	$N_{t+1}=N_t\exp(f(N_t))+\varepsilon_t$	$X_{t+1}=X_t+f(N_t)+\varepsilon_t$
Stepwise generalized logistic (SGL)	$N_{t+1}=F(1,N_t)+\varepsilon_t$	$X_{t+1}=\ln(F(1,N_t))+\varepsilon_t$

N_t is the census count at time t; $X_t=\ln(N_t)$; $F(t,\mathrm{N}_0)$ is the solution of the continuous-time generalized logistic (S1); $f=r[1-(N/K)^\theta]$ is the per capita growth rate of the generalized logistic; ε_t are independent $N(0,\sigma^2)$ variates

(pp. S16–S22). Due to further aging of the population and the eventual onset of density dependence, we restricted the application of the matrix model to the period December 1998 through December 2008 after introductions. Population vectors were compared using Keyfitz's Δ (Caswell 2001:101 and (S29)).

We adapted methods of Koons et al. (2005) to investigate transient dynamics in the model (pp. S30–S34). We projected the SKKR population vector for each December, 1998 through 2007, through two time steps to the following December, compared that projection with the SKKR population vector for the December to which the projection was made using Keyfitz's Δ, and computed the transient annual growth rate for each such projection as the ratio of projected population size to initial population size (the five exports during 2006 were retained for the comparison with the projection from 2005 to 2006). We also compared the rankings of sensitivities and elasticity of the transient growth rates to those of the asymptotic growth rate.

To directly investigate the influence of stage structure and stochasticity, the SKKR population vectors, augmented by the matrix-model projections of the five rhinoceros removed in May 2006, were compared to the matrix-model projections, through December 2008, of the population structure in December 1998, after introductions had ceased.

Engen et al. (2005) provided a formulation of stochasticity for structured populations. In particular, from the deterministic (female only) projection matrix A underlying the dynamics of a population of long-lived vertebrates that produce only a single offspring per breeding occasion, assuming no relationship between reproduction and subsequent adult survival and no environmental stochasticity, which turned out to be the case for our study population, one has

$$\sigma_d^2=\frac{1}{\lambda^2}\sum_{i,j}(\nu_i)^2u_ja_{ij}\left(1-a_{ij}\right) \tag{4}$$

where the summation is over non-zero entries of the projection matrix $A=(a_{ij})$, (u_i) is the stable-stage distribution of the female-only matrix model, and (ν_i) is the reproductive value vector, normalized to satisfy $\sum_i \nu_i u_i = 1$. Since our matrix model was constructed with a semi-annual time step, we applied Eq. (4) to $Z=A^2$, which is the projection over 1 year.

Results

Scalar models

Table 2 records the comparisons of the models in Table 1 for the semi-annual censuses. The discrete-time exponential was unambiguously the best model of the data for both error structures. While estimates of r were relatively consistent across models and precise, estimates of K and θ were not. For CGL, DGL, genRicker, and SGL and both error structures, estimates of K fell in the interval (110, 200) and for θ were greater than one but coefficients of variation (CVs) for both were large, at least 0.8 and often exceeding 10.

For additive error, the deviance of the CGL models with fixed θ fluctuated slightly for values of θ up to ten and then increased monotonically with θ (values ranging from 191.9 to 194.9), while for multiplicative error, the deviance increased monotonically with θ (values ranging from −106.0 to −99.6). Estimates of K for CGL with fixed θ, for both error structures, decreased monotonically with θ converging on 110, with CVs also decreasing to less than 0.1. For the SGL with fixed θ, for both error types, deviance did not vary with θ, but while estimates of K roughly decreased to near 110 with increasing θ, their CVs did not and were consistently much greater than one.

Differences in ΔAIC_c values amongst the discrete-time models in Table 2 were due almost entirely to the number of model parameters. The CGL models with fixed θ had ΔAIC_c similar to the other continuous-time models and so were not at all competitive. The SGL models with fixed θ, having only slightly larger deviance than the discrete-time exponential and only one more parameter, were competitive with ΔAIC_c values of about 2.3 (additive error) and 1.5 (multiplicative error) but did not, as noted above, yield informative estimates

Table 2 Results of non-linear regression of scalar models in Table 1 for the semi-annual census data

	Additive error					Multiplicative error				
Model	R^2	Dev	k	r±SE	ΔAIC_c	R^2	Dev	k	r±SE	ΔAIC_c
Cexp	0.996	194.9	2	0.0912±0.0023	25.6	0.995	−99.4	2	0.1016±0.0043	30.4
CGL	0.996	194.1	4	0.0921±0.0027	29.5	0.996	−106.3	4	0.115±0.011	28.3
Dexp	0.998	169.3	2	0.1017±0.0092	0	0.997	−129.9	2	0.102±0.017	0
DGL	0.998	169.3	4	0.106±0.021	4.7	0.997	−129.9	4	0.105±0.021	4.7
genRicker	0.998	169.3	4	0.103±0.020	4.7	0.997	−129.9	4	0.102±0.020	4.7
SGL	0.998	169.3	4	0.103±0.020	4.7	0.998	−130.7	4	0.102±0.020	3.9

Model name abbreviations as in Table 1; R^2 is 1− (ratio of error sum of squares to total sum of squares) for the regression fit; Dev is the deviance, −2 times the maximized log-likelihood; k is the number of estimable model parameters (including the variance of the residuals); r±SE is the estimated value of the parameter r common to all the models as an *annual* rate±its SE; ΔAIC_c is the model's AIC_c value minus that of the model with the smallest AIC_c value, which was the discrete-time exponential model in both analyses

of K. The model of Dennis et al. (1991) reproduced the estimate of r and its standard error (SE) for the discrete-time exponential with multiplicative error (their μ), gave a lower deviance than any model with additive error, and was almost 10 AIC_c units below the discrete-time exponential model and thus unambiguously the best model.

The most important difference between the analyses of the semi-annual census data and the annual (December) census data was that the latter favoured the naïve continuous-time models over the discrete-time models (Table S1). Although exponential growth was the top model for additive error, the CGL with θ=1 gave the best fit for multiplicative error (Fig. S4).

Matrix model

As the two parametrizations of the matrix model produced very similar results, we present the results for MM1 only (see pp. S23–S29 for MM2). From December 1999 to December 2008, Keyfitz's Δ between the matrix-model projections from December 1998 and the model stable-stage distribution strictly decreased from 0.227 to 0.001 (Fig. 2). Keyfitz's Δ between the annual projections to a given December, 1999–2008, and that December's SKKR population vector averaged (±SD) 0.054 (±0.025) with a low of 0.020 for the projection from 2003 to 2004 (Fig. S5). The corresponding projected (transient) growth rates over 1 year averaged (±SD) 1.1111 (±0.0084), ranging from 1.0967 to 1.1267 (Table S6), as compared to the asymptotic annual growth rate of λ=1.1078. Transient dynamics of the model were mild as the dependence on the initial population vector was erased. The rankings of sensitivities and elasticity were similar for both transient and asymptotic growth rates (Table S7).

The SKKR population vectors, December 1999 through December 2008, deviated somewhat from matrix-model projections (Table 3) and Keyfitz's Δ between the SKKR population vectors and both the corresponding matrix-model projections and stable-stage distribution exhibited mild fluctuations (Fig. 1). The discrepancies between the SKKR population vectors and the projections could be attributed to the differences between actual sex-specific annual recruitment and those of the model projections (Table 3; pp. S29–S30).

Process noise

The estimates of the demographic (σ_d^2) and environmental (σ_e^2) stochasticity from the unstructured population using the discrete-time model of exponential growth were 0.127 (of which 86 % were directly due to variation in fecundity as opposed to survival) and 0.0002, respectively. For the annual estimates from which these weighted means were obtained, the t test returned $p=10^{-6}$ and 0.44, respectively. The assumption that $\sigma_e^2=0$ for the application of Eq. (4) was consistent with this result. The resulting estimate of σ_d^2 from the female-only matrix model was 0.204.

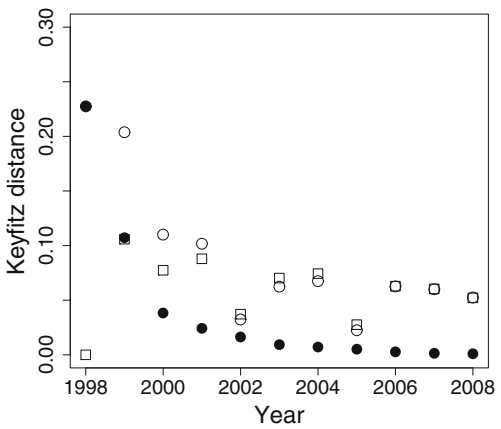

Fig. 2 Keyfitz's Δ between matrix-model projections (MMPs) from December 1998 and the model stable-stage distribution (*black circle*), the MMPs and the SKKR population vectors (*white square*), and the SKKR population vectors and the stable-stage distribution (*white circle*)

Table 3 The first column gives the year and Keyfitz's Δ between the SKKR population vector, listed in column 3, and the matrix-model projected population vector, listed in column 2

Year Δ	MM	SKKR	Recruits	Year Δ	MM	SKKR	Recruits
1999 0.1059	5.6 9.4 11.6 5.0 9.4 5.5	6 13 9 3 10 5	3.1 2.4 4 0	2004 0.0743	10.7 12.2 22.0 8.5 11.6 13.4	13 11 23 7 8 15	5.0 3.9 5 3
2000 0.0774	7.2 8.0 14.6 5.9 9.1 7.3	7 9 12 3 9 6	3.6 2.8 1 0	2005 0.0276	11.8 13.5 24.4 9.4 12.7 15.0	12 13 24 10 10 15	5.5 4.3 4 6
2001 0.0879	8.1 8.5 16.4 6.5 9.1 9.1	6 9 17 7 12 6	3.7 2.9 4 7	2006 0.0628	13.1 14.9 27.1 10.4 13.8 16.7	12 18 27 14 10 17	6.1 4.8 8 7
2002 0.0372	8.9 9.6 18.2 7.1 9.8 10.5	7 9 18 7 8 10	4.1 3.2 3 0	2007 0.0604	14.6 16.5 30.0 11.6 15.2 18.6	12 18 29 16 14 16	6.8 5.3 9 5
2003 0.0703	9.7 10.9 20.0 7.8 10.6 11.9	12 10 20 7 7 14	4.5 3.5 7 4	2008 0.0522	16.2 18.2 33.3 12.8 16.8 20.7	16 20 32 14 20 16	7.5 5.9 3 6

Projections are from the SKKR population in December 1998, and population vectors for a given year are for December of that year. The column headed 'Recruits' lists the projected number of female and male recruits, in that order, followed by the actual number of female and male recruits, in that order, to the population for the corresponding year ('recruits' being offspring of the year that survive to the end of the year; for the SKKR population, the probability of death in the first year after birth was negligible, so recruits are essentially births)

Discussion

Consistent with Nelder (1961), when fitting versions of the generalized logistic, estimates of K and especially θ were poor, often useless. Exponential growth can be mimicked by the generalized logistic with large values of K and/or θ, resulting in redundancy of these parameters when fit to exponential-growth-like data. The generalized logistic will be unreliable for modelling time series of abundance values only near K (Polansky et al. 2009; Clark et al. 2010) or only prior to pronounced density dependence (our study) but appears to be useful for data across the range of population growth (Eberhardt et al. 2008).

The semi-annual census data were unambiguously best fit by the discrete-time exponential model with multiplicative error amongst the models of Table 1. This model has the same likelihood as the model of Dennis et al. (1991) and the continuous-time stochastic exponential growth model (Tuckwell 1974). One expects process noise to be multiplicative on population growth if it is additive on vital rates (Turchin 2003:184). The non-competitive performance of the naïve continuous-time exponential growth model indicated that process noise contributed to the dynamics. But, the naïve continuous-time models were favoured over the discrete-time exponential model for the annual census data. Residuals of the fit of models indicated that differences between the results for the two time steps were an artefact of the annual time step rather than biologically informative (Figs. S1 and S2). It appears that stochasticity contained in the semi-annual censuses tended to average out over the annual

interval. Hence, censuses limited to longer intervals can misrepresent the dynamics of populations with asynchronized reproduction and no natural time step.

For annual survey data for two black rhinoceros populations that exhibited levelling off of population size, Cromsigt et al. (2002) employed discrete-time models with additive error (interpreted as observation error) and obtained good fits to their data with the DGL with estimates for θ of 10 and 28 (no SEs reported). Okita-Ouma et al. (2010) followed the procedure of Cromsigt et al. (2002) but found that only the exponential model returned sufficiently precise estimates of model parameters for three black rhinoceros populations. The time frame for both studies was roughly 10 years. Chamaillé-Jammes et al. (2008) used AIC_c to compare several discrete-time scalar models of population dynamics with multiplicative error, including the genRicker, for aerial survey counts of an elephant (*Loxodonta africana*) population exhibiting several years of considerable growth after cessation of culling, followed by fluctuations, and obtained the genRicker as best fit with θ=6.55 (SE=2.51) but ultimately found that only a model with K related to rainfall adequately explained their data. We propose that an extended period of exponential growth is common for expanding populations of megaherbivores. In addition to the SKKR population and those of Okita-Ouma et al. (2010), Knight et al. (2001) and Gough and Kerley (2006) reported exponential growth for expanding populations of black rhinoceros and elephant, respectively, while Brodie et al. (2011) deduced density-independent vital rates from mark-recapture survey data for a black rhinoceros population recovering from poaching.

Our estimate of the annual intrinsic rate of growth for the SKKR population (0.102±0.017) is at the high end of published values (Owen-Smith 1988; Knight et al. 2001; Okita-Ouma et al. 2010; Brodie et al. 2011; Ferreira et al. 2011; Greaver et al. 2014), which are typically below 0.1. Our estimate is within theoretical expectations based on the scaling law $r=1.5W^{-0.36}$ (Caughley and Krebs 1983), where W is the mean adult live weight in kilograms, 700–1400 for black rhinoceros (Owen-Smith 1988; 1000 kg yields r=0.125).

The matrix-model projection of the SKKR population vector for December 1998 converged monotonically and initially quite rapidly on the matrix model's stable-stage distribution (Fig. 2). Transience in the SKKR dynamics was also mild. Once reintroductions ceased, the deterministic dynamics implied that the SKKR population should approach its stable-stage distribution within the lifespan of black rhinoceros. If these results are typical for black rhinoceros, then transient dynamics will largely reflect unusual population structure rather than the subdominant eigenvalues. Nevertheless, the computation of projected annual growth rates could provide a useful tool for managers planning a removal, e.g., to check for rates below the asymptotic rate, which suggest less robust population structures.

The actual SKKR population vectors, December 1999 through December 2008, differed from the matrix-model projections and did not converge monotonically on the model's stable-stage distribution, exhibiting instead small fluctuations (Fig. 2). Similarly, Keyfitz's Δ between the annual projections of the SKKR population vectors for each December, 1998–2007, and the SKKR population vectors for the following December, though typically less than 0.1, did not converge on zero over this period (Fig. S5 and S6). Direct examination of the structured population trajectories and matrix projections (Table 3) indicated that the discrepancies could largely be attributed to deviations between the actual numbers of and model projections of sex-specific recruitment each year. We previously (Law et al. 2013, 2014) found no deterministic explanation for the variation in interbirth intervals or birth sex in the SKKR population and proposed that the variation was due to demographic stochasticity.

As measured by R^2 (Table 3), the fit of the scalar models to the abundance data was extremely high, yet the better fit of the discrete-time exponential model compared to the continuous-time model indicated the presence of process noise in the dynamics. From the unstructured population, we estimated environmental stochasticity to be negligible. The climate of the study area is warm temperate (Fike 2011) with rainfall expected to be the main driver of environmental influence on dynamics. Yet, we (Law et al. 2013, 2014) found no evidence for the influence of rainfall on interbirth intervals, age at first reproduction, or birth sex, consistent with our estimation of no environmental stochasticity.

There have been few estimates of demographic stochasticity for long-lived vertebrates or mammals. For the unstructured population, our estimate of 0.127 compares with values of 0.267 for a population of Swiss ibex (*Capra ibex*) (Sæther et al. 2007b), 0.28 for the Soay sheep (*Ovis aries*) of Hirta Island, UK (Lande et al. 2003, Table 1.2), 0.571 for Scandinavian wolverines (*Gulo gulo*) (Sæther et al. 2005), and 0.745 for a population of Norwegian roe deer (*Capreolus capreolus*) (Grøtan et al. 2005). For structured population models, our estimate of 0.204 compares with 0.084 for a population of wandering albatross (*Diomedea exulans*) (Engen et al. 2005), 0.15 for a Norwegian island population of moose (*Alces acles*) using the method of Engen et al. 2005 (Sæther et al. 2007a), and 0.155 and 0.180 for two populations of Scandinavian brown bear (*Ursus arctos*) (Sæther et al. 1998b). The studies of Sæther et al. (1998b, 2007a, 2007b) also reported very low (<0.008) to negligible values for environmental stochasticity. Our estimates of demographic stochasticity are similar to those for species with long generation times (Sæther et al. 2007a). The larger values obtained in the studies cited above appear to result from a combination of high adult survival and variable recruitment, the SKKR population also exhibiting high adult survival but more modest variable recruitment. The

absence of environmental stochasticity and moderate demographic stochasticity implies that the mean of observed $\ln(N_{t+1}/N_t)$ values should not be much less than the intrinsic rate of growth, which no doubt aided the success of this reintroduction. Unlike SKKR, calf mortality was important in the studies of Hrabar and du Toit (2005), Brodie et al. (2011), and Greaver et al. (2014) and may be components of environmental and/or demographic stochasticity and/or the deterministic dynamics of those populations.

For megaherbivores, an extended period of exponential growth consistent with the threshold model of McCullough (1992, 1999), employed by Emslie (2001) for rhinoceros meta-population management, may be common. It remains unclear, however, at what rate population growth declines when density feedback begins. We previously reported (Law et al. 2013) an increase of age at first reproduction in SKKR with increasing population size despite no apparent resource limitation (van Lieverloo et al. 2009) and suggested that this response may be socially mediated (Bronson 1989:163). Increase in age at first reproduction might therefore provide a practical early warning sign of density feedback in an expanding population of megaherbivores prior to detectable slowing in growth rate. Further study across populations and species is required to explore this possibility. Process noise was present in the SKKR dynamics, identified as variation primarily in recruitment. Demographic stochasticity is likely important for understanding megaherbivore population dynamics, as such populations are often relatively small, and therefore of relevance to the impact of removals both on donor populations and on the performance of reintroduced populations. Though megaherbivores may exhibit some robustness to environmental variation, e.g., Brodie et al. (2011:355) also found no temporal variation in vital rates over a 14-year period in a black rhinoceros population, we would expect environmental stochasticity to be common, as in Gough and Kerley (2006), Hrabar and du Toit (2005) Chamaillé-Jammes et al. (2008), and Lee et al. (2011).

Acknowledgments Our collaboration is a by-product of an International Science Liaison Foreign Fellowship, National Research Foundation, Republic of South Africa, PRL shared with W. Linklater (WL) in 2005. We thank WL, for his pivotal role in obtaining this fellowship, bringing the three authors together, and for ongoing dialogue on rhinos, G. Kerley, for hosting WL and PRL during their fellowship at the Centre for African Conservation Ecology, Nelson Mandela Metropolitan University, and the SKKR field rangers.

References

Armstrong DP, Seddon PJ (2007) Directions in reintroduction biology. Trends Ecol Evol 23:20–25

Bonenfant C, Gaillard J, Coulson T, Festa-Bianchet M, Loison A, Garel M, Loe LE, Blanchard P, Pettorelli N, Owen-Smith N, Du Toit J, Duncan PK (2009) Empirical evidence of density-dependence in populations of large herbivores. Adv Ecol Res 41:314–357

Brault S, Caswell H (1993) Pod-specific demography of killer whales (*Orcinus orca*). Ecology 74:1444–1454

Brodie JF, Muntifering J, Hearn M, Loutit B, Loutit R, Brell B, Uri-Khob S, Leader-Williams N, du Preez P (2011) Population recovery of black rhinoceros in north-west Namibia following poaching. Anim Conserv 14:354–362

Bronson FH (1989) Mammalian reproductive biology. University of Chicago Press, Chicago

Burnham KP, Anderson DW (2002) Model selection and multimodel inference: a practical information-theoretic approach, 2nd edn. Springer, New York

Caswell H (2001) Matrix population models: construction, analysis, and interpretation, 2nd edn. Sinauer, Sunderland

Caughley G, Krebs CJ (1983) Are big mammals simply little mammals writ large? Oecologia 59:7–17

Chamaillé-Jammes S, Fritz H, Valeix M, Murindagomo F, Clobert J (2008) Resource variability, aggregation and direct density dependence in an open context: the local regulation of an African elephant population. J Anim Ecol 77:135–144

Clark F, Brook BW, Delean S, Akçakaya HR, Bradshaw CJA (2010) The theta-logistic is unreliable for modelling most census data. Methods Ecol Evol 1:253–262

Cromsigt JPGM, Hearne J, Heitkönig IMA, Prins HHT (2002) Using models in the management of black rhino populations. Ecol Model 149:203–211

Dennis B, Munholland PL, Scott JM (1991) Estimation of growth and extinction parameters for endangered species. Ecol Monogr 61:115–143

deValpine P, Hastings A (2002) Fitting population models incorporating process noise and observation error. Ecol Monogr 72:57–76

Eberhardt LL, Breiwick JM, Demaster DP (2008) Analyzing population growth curves. Oikos 117:1240–1246

Emslie RH (ed) (2001) Proceedings of a SADC Rhino Management Group (RMG) workshop in biological management to meet continental and national black rhino conservation goals. Giants Castle, 24–26 July 2001

Emslie RH, Amin R, Kock R (2009) Guidelines for the *in situ* reintroduction and translocation of African and Asian rhinoceros. Occasional Paper of the IUCN Species Survival Commission No. 39. IUCN, Switzerland, 115 pp

Engen S, Lande R, Sæther B-E, Weimerskirch H (2005) Extinction in relation to demographic and environmental stochasticity in age-structured models. Math Biosci 195:210–227

Ferreira SM, Greaver CC, Knight MH (2011) Assessing the population performance of the black rhinoceros in Kruger National Park. S Afr J Wildl Res 41:192–204

Fike B (2011) The demography and population dynamics of a reintroduced black rhinoceros population on the Great Fish River Reserve, Eastern Cape Province. M.Sc. thesis, Rhodes University

Fowler CW (1981) Density dependence as related to life history strategy. Ecology 62:602–610

Fowler CW (1987) A review of density dependence in populations of large mammals. In: Genoways HH (ed) Current mammalogy, vol 1. Plenum, New York, pp 401–441

Freckleton RP, Watkinson AR, Green RE, Sutherland WJ (2006) Census error and the detection of density dependence. J Anim Ecol 75:837–851

Ganqa NM, Scogings PF (2007) Forage quality, twig diameter, and growth habit of woody plants browsed by black rhinoceros in semi-arid subtropical thicket, South Africa. J Arid Environ 70:514–526

Ganqa NM, Scogings PF, Raats JG (2005) Diet selection and forage quality factors affecting woody plant selection by black rhinoceros

in the Great Fish River Reserve, South Africa. S Afr J Wildl Res 35: 77–83

Goodman LA (1969) The analysis of population growth when the birth and death rates depend upon several factors. Biometrics 25:659–681

Gough KF, Kerley GIH (2006) Demography and population dynamics in the elephants *Loxodonta africana* of Addo Elephant National Park, South Africa: is there evidence of density dependent regulation? Oryx 40:434–441

Greaver C, Ferreira S, Slotow R (2014) Density-dependent regulation of the critical endangered black rhinoceros population in Ithala Game Reserve, South Africa. Austral Ecol 39:437–447

Grøtan V, Sæther B-E, Engen S, Solberg EJ, Linnell JDC, Andersen R, Brøseth H, Lind E (2005) Climate causes large scale spatial synchrony in population fluctuations of a temperate herbivore. Ecology 86:1472–1482

Hrabar H, du Toit JT (2005) Dynamics of a protected black rhino (*Diceros bicornis*) population: Pilanesberg National Park, South Africa. Anim Conserv 8:259–267

Knight MH, Kshatriya M, Van Jaarveld AS, Nicholls AO, Hall-Martin AJ (2001) Evaluating herbivore extinction probabilities in Addo Elephant National Park, South Africa. Afr Zool 36:13–22

Koons DN, Grand JB, Zinner B, Rockwell RE (2005) Transient population dynamics: relations to life history and initial population size. Ecol Model 185:283–297

Lande R, Engen S, Sæther B-E (2003) Stochastic population dynamics in ecology and conservation. Oxford UP, New York

Law PR, Linklater WL (2014) Black rhinoceros demography should be stage, not age, based. Afr J Ecol 52:571–573. doi:10.1111/aje.12148

Law PR, Fike B, Lent PC (2013) Mortality and female fecundity in an expanding black rhinoceros (*Diceros bicornis minor*) population. Eur J Wildl Res 59:477–485

Law PR, Fike B, Lent PC (2014) Birth sex in an expanding black rhinoceros (*Diceros bicornis minor*) population. J Mammal 95:349–356

Lee PC, Lindsay WK, Moss CJ (2011) Ecological patterns of variability in demographic rates. In: Moss CJ, Croze H, Lee PC (eds) The amboseli elephants: a long term perspective on a long lived mammal. University of Chicago Press, Chicago, pp 74–88

Lent PC, Fike B (2003) Home ranges, movements and spatial relationships in an expanding population of black rhinoceros in the Great Fish River Reserve, South Africa. S Afr J Wildl Res 33:109–118

McCullough DR (1992) Concepts of large herbivore population dynamics. In: McCullough DR, Barrett RG (eds) Wildlife 2001: populations. Elsevier, Barking, pp 967–984

McCullough DR (1999) Density dependence and life-history strategies of ungulates. J Mammal 80:1130–1146

Morris WF, Doak DF (2002) Quantitative conservation biology: theory and practice of population viability analysis. Sinauer, Sunderland

Nelder JA (1961) The fitting of a generalization of the logistic curve. Biometrics 17:89–110

Okita-Ouma B. (2014) Population estimates of eastern black rhinoceros: unravelling the controls. PhD thesis, Wageningen University

Okita-Ouma B, Amin R, van Langevelde F, Leader-Williams N (2010) Density dependence and population dynamics of black rhinos (*Diceros bicornis michaeli*) in Kenya's rhino sanctuaries. Afr J Ecol 48:791–799

Owen-Smith RN (1988) Megaherbivores: the influence of very large body size on ecology. Cambridge UP, Cambridge

Owen-Smith N (ed) (2010) Dynamics of large herbivore populations in changing environments: towards appropriate models. Wiley-Blackwell, Chichester

Polansky L, de Valpine P, Lloyd-Smith JO, Getz WM (2009) Likelihood ridges and multimodality in population growth rate models. Ecology 90:2313–2320

Sæther B-E, Engen S, Islam A, McCleery R, Perrins C (1998a) Environmental stochasticity and extinction in a population of a small songbird, the great tit. Am Nat 151:441–450

Sæther B-E, Engen S, Swenson JE, Bakke Ø, Sandegren F (1998b) Assessing the viability of Scandinavian brown bear, *Ursus arctos*, populations: the effects of uncertain parameter estimates. Oikos 83: 403–416

Sæther B-E, Engen S, Persson J, Brøseth H, Landa A, Willebrand T (2005) Management strategies for the wolverines in Scandinavia. J Wildl Manage 69:1001–1014

Sæther B-E, Engen S, Solberg EJ, Heim M (2007a) Estimating the growth of a newly established moose population using reproductive value. Ecography 30:417–421

Sæther B-E, Lillegågard M, Grøtan V, Filli F, Engen S (2007b) Predicting fluctuations of reintroduced ibex populations: the importance of density dependence, environmental stochasticity and uncertain population estimates. J Anim Ecol 76:326–336

Seddon PJ, Armstrong DP, Maloney RE (2007) Developing the science of introduction biology. Conserv Biol 21:303–312

Shenk TM, White GC, Burnham KP (1998) Sampling-variance effects on detecting density dependence from temporal trends in natural populations. Ecol Monogr 68:445–463

Tuckwell HC (1974) A study of some diffusion models of population growth. Theor Popul Biol 5:345–357

Turchin P (2003) Complex population dynamics. Princeton UP, Princeton

van Lieverloo RJ, Schuiling BF, de Boer WF, Lent PC, de Jong CB, Brown D, Prins HHT (2009) A comparison of faecal analysis with backtracking to determine the diet composition and species preference of the black rhinoceros (*Diceros bicornis minor*). Eur J Wildl Res 55:505–515

Supplementary Information for `Dynamics of an expanding black rhinoceros population' by Law, Fike and Lent. European Journal of Wildlife Research.

Corresponding author: Peter R. Law; prldb@member.ams.org.

Only citations not appearing in the main text are listed under References at the end of the Supporting Information.

INTRODUCTION

The Generalized Logistic

The generalized logistic can be solved in the same manner as the logistic, integrating using partial fractions, or one can simply put $M = N^{\theta}$, $J = K^{\theta}$, and $s = r\theta$ and the generalized logistic ODE becomes

$$\frac{M'}{M} = s\left(1 - \frac{M}{J}\right),$$

i.e., the logistic equation for these quantities. Hence, the solution of the generalized logistic can be obtained directly from the well-known solution of the logsitic as

$$N(t) = \frac{N_0 e^{rt}}{\left[1 + \left(\frac{N_0}{K}\right)^{\theta}\left(e^{r\theta t} - 1\right)\right]^{1/\theta}} = \frac{K}{\left[1 + \left(\left(\frac{K}{N_0}\right)^{\theta} - 1\right)e^{-r\theta t}\right]^{1/\theta}}. \qquad \text{(S1)}$$

From (S1), one sees that for $N_0 << K$ and so that $(N_0/K) < e^{-rt}$, then for large θ the denominator in the first form is approximately one and $N(t)$ behaves as exponential growth over that range of t values. Yet the solution still converges on the equilibrium K for large t and does so rapidly once the rate of growth begins to decline. Indeed, as $\theta \to \infty$, the solution converges on exponential growth until $N(t)$ reaches K and growth ceases, which is an extreme form of threshold model. McCullough (1999) proposed that per capita growth rate (pgr) might remain constant from low abundance to near equilibrium (corresponding to exponential growth) and then decline rapidly as equilibrium is approached. For such a model, $N(t)$ is continuous but only piecewise differentiable, with a point of nondifferentiability at the threshold value N^* at which exponential growth ceases. If the decline is modelled by the generalized logistic, then the expression for $N(t)$ is an exponential growth curve joined at N^* to a solution of the generalized logistic with the same r and suitable θ and K (see also Owen-Smith 2010:39). Taking $\theta = 1$ gives linear decline in pgr after the threshold, sometimes called the 'ramp' model.

The graph of (S1) is sigmoid with point of inflexion at

$$N_H = \frac{K}{\sqrt[\theta]{1+\theta}}. \qquad \text{(S2)}$$

N_H is also the abundance at which population growth rate $N'(t)$ is a maximum. For $\theta > 1$, $N_H > K/2$ and approaches K as $\theta \to \infty$. Hence, for $\theta > 1$, the abundance for optimal sustainable harvesting is nearer to K than the value of $K/2$ for the logistic. For a threshold model of population growth, optimal sustainable harvesting can be achieved by harvesting at the model's threshold value N^*. Thus, the appropriate model of population dynamics informs not only how the population approaches equilibrium but also how removals can be undertaken to source new populations.

METHODS

The Study Population and Dataset

Thirteen males and 15 females were introduced but 3 males and 2 females died soon after release and did not contribute to the population. The surviving imports included only two females and two males that were already adults. For details of the introductions can be found in Fike (2011). One further individual, a female adult, entered the SKKR population, from the eastern sector of the Great Fish River Nature Reserve (GFRR), in 2003. This immigrant was the only exception to the demographic isolation of the SKKR population during the study period. She calved for the first time after entering the SKKR population and is included as a member of the SKKR population from her time of entry.

The export of 1 SA male and 4 SA females in May 2006 yielded a sex ratio of 9:10 as a result of imports and exports, after discounting the failed imports. Our demographic study of the SKKR population focused on the period from reintroduction through the end of 2008 to obtain the longest study period possible with minimal effects from removals. As explained below, the removals were accounted for in the analyses of this paper for both scalar and matrix models, though in different ways. More substantial removals were conducted after 2008.

The complete absence of poaching in the GFRR, the fact that only five rhinos were removed prior to 2009 by management, and the excellent monitoring of the population at the individual level made this population an excellent opportunity for the study of black rhino ecology in general and the performance of a reintroduced population in particular.

As each individual of the SKKR population was ear notched, routine monitoring and recording of all births and deaths resulted in a record of the population over time, allowing actual population censuses to be computed for any month from Jun-86 through Dec-08. The only uncertainty in such censuses arises from uncertainties in birth and death dates. At the initial recording of each birth and death, an interval of uncertainty was assigned to reflect the precision of the birth or death date (Fike 2011). The interval of uncertainty, in months, centered on the nominal birth date (d), was specified by a value U so that the interval of uncertainty was $d - U$ to $d + U$. The values of U employed by Fike (2011) were: $U = 0$ (uncertainty in the nominal date at most 1 week); $U = 1$; $U = 3$; $U = 6$; $U = 12$; $U > 12$. For 106 births and 15 deaths, 29 had $U = 0$, 38 had $U = 1$, 32 had $U = 3$, 20 had $U = 6$, 2 had $U = 12$, and none had $U > 12$. We therefore computed censuses semi-annually, every June and

December to limit the effects of these uncertainties. We then used the assigned intervals of uncertainties to inspect their impact on the censuses by noting when a rhino was unambiguously present or not and counting the **maximum** possible number of rhino that might be added to or subtracted from the nominal census count due to the uncertainty of birth and death dates. Expressed as percentages of the nominal census counts, only three possible modifications exceeded 10%, each at very low population levels (viz., an ambiguity of one rhino in a count of three or four). From Jun-86 through Jun-98, 17 of 25 censuses possessed no ambiguity at all. From Dec-98 through Dec-08, an ambiguity was always present but in 14 of 21 censuses was less than 5%. It was clear that this data could not be modelled as independently and identically distributed. As these were maximum estimates of uncertainty, and ambiguous presence and ambiguous absence, when both present, would tend to cancel, taking the nominal censuses as actual population censuses seemed plausible.

Since the data does not indicate an equilibrium or obvious threshold, we could not include a threshold model amongst the candidate models, e.g.., a model based on the ODE of the form

$$\frac{N'}{N} = \begin{cases} r, N \le N_* \\ r\left(\dfrac{K-N}{K-N_*}\right), N \ge N_* \end{cases} \qquad \text{(S3)}$$

in which it is assumed that N_* is close to K, but threshold-like dynamics can be approximated by large values of θ in the generalized logistic.

Error Structure and Process Noise

To illustrate the differences between deterministic and stochastic, and between continuous- and discrete-time, models, consider exponential growth. First note that in the absence of stochasticity,

$$N_t = N_0 e^{rt} = N_0 e^{r[1+(t-1)]} = e^r N_{t-1} \qquad \text{(S4)}$$

i.e., the continuous- and discrete-time models agree. Suppose there is a single stochastic perturbation to the population at time $s < t$. The discrete-time model incorporates this perturbation at the step following the perturbation and future projections incorporate this perturbation and are thus accurate. The naïve continuous-time model, however, continues to project future population size from the initial population size N_0 and thus will differ from the actual population size at all times greater than and equal to s. Thus, the discrete time model will have just the one residual error when fit to actual population size while the naïve continuous-time model will have residuals for all times greater than or equal to s. Hence, the naïve continuous-time model can only be expected to provide a good fit to data in the absence of stochasticity or perhaps when the stochasticity in the data is small and tends to cancel out over time. In effect the naïve continuous-time model does not see stochasticity but the discrete-time model does even if $N_s = e^r N_{s-1} + e$ ($e > 0$, say) but $N_{s+1} = e^r N_s - d$ ($d > 0$).

A more realistic approach to continuous-time dynamics with process noise was initiated by Levins (1969), who wrote $N'/N = r(t)$ with solution

$$N(t) = N_0 \exp\left[\int_0^t r(s)ds\right] \qquad \text{(S5)}$$

and applied the central limit theorem to the integral to deduce that it approaches a normal variate, whence $N(t)$ is log-normally distributed. More formally, one replaces a deterministic ODE by a stochastic differential equation (SDE), in which specific parameters (e.g., r and/or K) are treated as stochastic variables (e.g., Tuckwell 1974, but there is an extensive literature on continuous-time stochastic processes and SDEs). For exponential growth, the ODE $N'/N = r$, r constant, becomes $N'/N = r(t) = r + \varepsilon(t)$, which is formalized by the SDE

$$dN = rN(t)dt + \sigma N(t)dW(t) \qquad \text{(S6)}$$

in which $\varepsilon(t)dt$ has been replaced by $\sigma dW(t)$, with $dW(t)$ representing the 'differential' of the Wiener process, representing Gaussian 'white' noise. For a likelihood model of the stochastic process described by an SDE, one requires the probability density $p(N_t,t,|N_{t-1})$ of observing abundance N_t at time t given that the abundance at time t-1 was N_{t-1}. This probability density is obtained as the solution to the Fokker-Planck equation. When solvable, the solutions are typically analytically complicated.

Given our data, the discrete-time models should suffice to detect density dependence if present in our data. As the SKKR population did not manifest fluctuations, more complex models of stochastic dynamics appear unnecessary for our purpose. We do note, however, that for continuous-time, stochastic exponential growth, the resulting $p(N_t,t,|N_{t-1})$ is log-normal and the expected abundance obeys deterministic exponential growth but with a coefficient of variation that increases exponentially as $t \to \infty$ (Tuckwell 1974). The discrete-time exponential model with multiplicative error is

$$X_t = X_{t-1} + r + \varepsilon_{t-1} \text{ whence } X_t = X_0 + rt + \sum_{j=0}^{t-1} \varepsilon_j = X_0 + rt + \varepsilon \qquad \text{(S7)}$$

where ε is a sum of iid $N(0,\sigma^2)$ variates and thus $N(0,\sigma^2 t)$. Hence, X_t is $N(X_0 + rt, \sigma^2 t)$, which includes the description of a single time step as 'X_t is $N(X_{t-1} + r, \sigma^2)$'. Thus the discrete-time exponential model generates the same likelihood for the data X_t as the model of Dennis *et al*. (1991; except that they use μ where we use r and their r differs from ours). Dennis *et al*. observed that these distributional assumptions for X_t are equivalent to $p(N_t,t,|N_{t-1})$ being log-normal. Hence, for a time series of abundances, the likelihood models obtained from the discrete-time exponential model with multiplicative error, from Dennis *et al*. (1991), and from the continuous-time stochastic exponential growth model are all identical, i.e., such a time series cannot distinguish these models. Moreover, since Dennis *et al*.'s model employs N_t, rather than X_t, as the response variable, its likelihood model of the time-series data can be compared via AIC_c to the models of Table 1 with additive error, thereby providing a common

reference between the comparisons of the additive error models plus Dennis *et al.*'s model and the comparisons of the multiplicative error models (via the discrete-time exponential model).

Thus, we consider the models listed in Table 1, together with the model of Dennis et al. (1991) with N_t as response and thus with error additive on abundance, as adequate for our purposes of checking for density dependence and preferred error structure. Finally, we note that the statistical assumptions regarding residuals in nonlinear regression, see below, entail that the residuals as process noise are typically interpreted as representing environmental stochasticity, which is not say that demographic stochasticity is absent from the data. Rather, more than fitting the data to such models is required to determine the nature of process noise if present in the data. We address this issue in subsequent analyses below.

Including Additions and Removals in Population Modelling

All introduction events were sufficiently discrete to have occurred between two consecutive semi-annual censuses. In our case there was just the one removal event and no additions occurred during the semi-annual period of Dec-06 to Jun-06 when the removals were conducted. For discrete-time models, if n is the net number of individuals added (with negative values of n accounting for a net number of removals) between t and t+1, then the model projection from N_t should be compared to $M_{t+1} := N_{t+1} - n$ rather than N_{t+1} itself. Thus, for discrete time models, the modified census figures M_t were used as the response variable in the nonlinear regressions with additive error and $Y_t := \ln(M_t)$ was used for the response variable for models with multiplicative error. Thus, if the deterministic model is written as $N_{t+1} = G(N_t)$, then to accommodate additions and removals we use instead $M_{t+1} = G(N_t)$.

For the continuous-time models in Table 1, projections of future abundance are made via the solution of the ODE from an initial population size. In our case, there were 5 distinct addition events, including the immigration of the one female from the other half of GFRR into SKKR, after the founding introduction in Jun-86 and one removal event. The entire period of study can be partitioned into 7 disjoint subintervals of time $[0, t_1]$, $[t_1, t_2]$,…,$[t_6, t_7]$ such that each subinterval consists of several consecutive between-census periods and such that each distinct addition or removal event occurred in the final between-census period of one of the first six of these subintervals. Thus, $[0,t_1]$ covers the time period from time zero to the census immediately following the first addition; $[t_1, t_2]$ covers the period from t_1 to the census immediately following the next distinct addition event; and so on, except that $[t_6, t_7]$ covers the period from the census immediately following the final addition/removal (the removal in our case) to the final census. If F denotes the solution of the deterministic continuous-time model as in (3), then for the additive error models one uses: $F(t, N_0)$ to project abundance over $[0, t_1]$; $F(t - t_1,\ N_{t_1})$ to project abundance over $[t_1, t_2]$; and so on, finally using $F(t - t_6,\ N_{t_6})$ to project abundance over $[t_6, t_7]$. These projections are compared to the modified census figures M_t for each census time t. For the models with multiplicative

error, one projects abundances as just described, takes the logarithms of the projections, and compares to the Y_t.

We also needed to modify the likelihood formulae of Dennis *et al*. (1991) to accommodate additions and removals (as they apparently did in their example of the Puerto Rican parrot, see their p. 135). Dennis *et al*. formulated a stochastic model for (st)age structured exponentially growing populations with process noise that can be fitted to time series N_0, N_1,...N_q of abundances (censuses, not estimates), with time step τ_i from the (i-1)'th observation to the i'th observation. The likelihood is built from the probability $p(N_i, \tau_i|N_{i-1})$ of observing N_i at the i'th observation given that the abundance was N_{i-1} at the (i-1)'th observation. Let M_i := N_i + removals - additions (removals and additions during the time step from the (i-1)'th observation to the i'th observation) denote the modified count (as above). Then, in place of Dennis *et al*.'s $p(N_i, \tau_i|N_{i-1})$ we have $p(M_i, \tau_i|N_{i-1})$. In our case, the time steps are all equal. For the semi-annual censuses, τ_i = ½, for a time unit of one year, and q = 45, i.e., 45 observations (N_0,M_1),...,(N_{44}, M_{45}), each Jun and Dec from Dec-86 through Dec-08 and $t_q = \sum_{i=1}^{q} \tau_i$ = 45/2. For annual censuses, τ_i = 1, q = 22, with observations (N_0,M_1),...,(N_{21},M_{22}), from Dec-87 through Dec-08, and $t_q = \sum_{i=1}^{q} \tau_i$ = 22.

The probability $p(N_i, \tau_i|N_{i-1})$ was derived by Dennis *et al*. from a log-normal distribution with parameters μ and σ^2 (see their equation (8)) and the likelihood of the data (their (22)) by multiplying together such probabilities, one for each observation. Thus, to accommodate additions and removals, one literally replaces the N_i (but not N_{i-1}) in their formula by M_i. This substitution modifies the maximum likelihood estimates of μ and σ^2 obtained by Dennis *et al*. as follows. In place of their equations (24) and (25), one readily obtains

$$\hat{\mu} = \frac{\sum_{i=1}^{q} \ln\left(\frac{M_i}{N_i}\right)}{t_q} = \frac{\ln\left(\frac{M_1 \ldots M_q}{N_0 \ldots N_{q-1}}\right)}{t_q} \qquad \text{(S8)}$$

and

$$\hat{\sigma}^2 = \frac{1}{q}\sum_{i=1}^{q} \frac{\left[\ln\left(\frac{M_i}{N_{i-1}}\right) - \hat{\mu}\tau_i\right]^2}{\tau_i}, \qquad \text{(S9)}$$

respectively, with the latter simplifying in our case to

$$\hat{\sigma}^2 = \frac{1}{q\tau}\sum_{i=1}^{q}\left[\ln\left(\frac{M_i}{N_{i-1}}\right) - \hat{\mu}\tau\right]^2 \qquad \text{(S10)}$$

because of equal time steps. But nothing else changes for the analysis of Dennis *et al*. (1991) (though in the linear regression model one has $W_i = \ln(M_i/N_{i-1})$ of course; $\ln(M_i)$ is the modified value of $\ln(N_i)$ and thus W_i still represents the increments of the Wiener process, whence the statistical properties that Dennis *et al*. appeal to remain valid and the rest of their results apply). The maximized log-likelihood is (for equal time steps)

$$-\sum_{i=1}^{q} \ln\left[\sqrt{2\pi\tau} M_i\right] - \frac{q}{2}\left[1 + \ln\left(\hat{\sigma}^2\right)\right] \qquad \text{(S11)}$$

Note that, with $Y_t = \ln(M_t)$, $p(Y_t,1|X_{t-1})$ is $N(X_{t-1} + r,\ \sigma^2)$, just as in the discrete-time exponential model with multiplicative error, so the equivalence of the likelihood descriptions of a time series of abundances is maintained when introductions and removals are accounted for.

Nonlinear regression and AIC_c

For a model of the form

$$z_k = f(x_k) + \varepsilon_k \qquad \text{(S12)}$$

with ε_k iid $N(0,\sigma^2)$ and n observations, the log-likelihood is

$$\ln(L) = \sum_k \frac{-\left[z_k - f(x_k)\right]^2}{2\sigma^2} - (n/2)\ln(2\pi\sigma^2) = -\frac{RSS}{2\sigma^2} - (n/2)\ln(2\pi\sigma^2) \qquad \text{(S13)}$$

where *RSS* is the residual sum of squares (Burnham and Anderson 2002:12, 108–109; Bates and Watts 1988:4). Maximum likelihood (ML) estimation of the structural parameters in f is equivalent to (non-linear) least-squares estimation. ML estimation of σ^2 is found easily by calculus to be

$$\sigma^2_{\max} = \frac{RSS_{\max}}{n} \qquad \text{(S14)}$$

where $RSS_{\max}$ denotes the residual sum of squares evaluated for the ML estimates of the structural parameters of f (i.e., what is usually meant by the residual sum of squares). The deviance (i.e., -2 times the maximized log-likelihood) is then found to be

$$D = n\ln\left(\frac{RSS_{\max}}{n}\right) + n[1 + \ln(2\pi)] \qquad \text{(S15)}$$

Nonlinear regression was performed in the nonlinear estimation module of Statistica 8 (Statsoft), which provided the ML estimates of the structural parameters of the model and the residuals. From the residuals we computed $\sigma^2_{\max}$ and the deviance D. AIC_c was then computed as

$$\mathrm{AIC_c} = D + \frac{2nk}{n-k-1} \qquad \text{(S16)}$$

(Burnham and Anderson 2002), where k is the number of estimated parameters, here the number of structural parameters in the model plus one (for σ^2), and n is the number of data points used in the likelihood. Note that a time series of length one does not permit estimation for any of the models in Table 1, i.e., the initial population census does not count as a datum point in the likelihood. As noted above in the discussion of Dennis *et al*.'s model, the 23 years of Jun and Dec censuses yield 45 semi-annual census data of the form (M_{t+1}, N_t) and 22 annual census data of a similar form. Thus, for all models, n = 45 for the semi-annual census data and 22 for the annual census data.

For $\mathrm{AIC_c}$ calculations, the second term in (S15) is common to all nonlinear regression models so cancels out in computations of $\Delta\mathrm{AIC_c}$ for such models. However, for comparisons of the models with additive error with the model of Dennis *et al*. (1991) it is essential to retain that term in the deviance and all $\mathrm{AIC_c}$ calculations.

Statistica provides an R^2 value for each nonlinear regression, computed as follows. The total sum of squares (SS) is defined as usual for a response variable z as $\sum_j \left(z_j - \bar{z}\right)^2$ and the Error SS is defined as $\sum_j \left(z_j - \hat{z}_j\right)^2$, where $\hat{z}_j$ is the predicted value. Statistica then defines the regression SS as Total SS – Error SS and R^2 as the ratio of regression SS to total SS, i.e., as 1 – (the ratio of Error SS to Total SS), as a measure of variation explained by the model.

Nonlinear regression requires starting values (SV) for the structural parameters to be estimated (Bates and Watts 1988). For r we used 0.05 as SV for both semi-annual and annual census analyses, which proved unproblematic. For K we began with an SV of 150. Since the dataset gave no indication that an equilibrium population size had been reached, we expect K to be larger than 110 (mean density 0.5 rhino/sq. km), the Dec-08 census figure. The highest local density for black rhinoceros reported by Owen-Smith (1988:224) was 1.6 rhino/sq. kms. A mean density of 1.6 should therefore provide an upper bound on K, yielding 352. In fitting the generalized logistic with θ fixed, we found that we had to lower the SV of K as θ increased in order for Statistica to fit the model (otherwise it complained that the remaining model parameters were 'probably very redundant; estimates suspect'). Larger SVs for K did not help.

For large herbivores, one expects $\theta > 1$ (Owen-Smith 2010). This expectation appears to be challenged by Sibly et al. (2005), who fitted numerous time series of abundances from the Global Population Dynamics Database (GPDD; http://www3.imperial.ac.uk/cpb/databases/gpdd) to the generalized Ricker model with multiplicative error and obtained more often than not values of $\theta < 1$ and even negative. For critical assessments of these analyses and Sibly et al.'s response, see *Science* **311** (2006),

p.1100d, and further see Doncaster (2008), Eberhardt *et al*. (2008), Polansky *et al*. (2009), and Clark *et al*. (2010). The values of θ obtained by Sibly *et al*. are appended to the corresponding time series in the GPDD. Systematic inspection of all time series for Rhinocerotidae, Elephantidae, Giraffidae, Hippopotamidae, Bovidae, and Cervidae found little evidence to contradict the expectation of $\theta > 1$ for large herbivores. There were actually few such time series for which θ was estimated and for those time series from robust studies θ was estimated to be greater than one, except in the one case of Owen-Smith's (1990) study. But Owen-Smith found that fluctuations in abundance in that study were significantly influenced by exogenous factors in addition to density, which may have complicated estimates of θ. For models in which θ was to be estimated in our analyses, we tried SVs of 1 and 4.5 (the latter following Eberhardt *et al*. 2008). For the semi-annual censuses, for CGL with additive error, when SV was set to one, Statistica reported model parameters were 'probably very redundant; estimates suspect', but fit the model to the data with an SV of 4.5. The opposite was the case for the CGL with multiplicative error. The resulting estimates of θ of 11.3 and 1.3, respectively, may reflect a dependence on SVs due to the redundancy. Both estimates had high CV, 3.6 and 0.9, respectively. (In the case of multiplicative error, the estimate of K was essentially the same estimate as obtained for CGL with θ fixed at one.) For the DGL, genRicker, and SGL, estimates were obtained with both SVs for both error structures. An SV of 1 for θ either yielded the same result as an SV of 4.5 or an estimate for K greater than 1000, which is unrealistically high, and an estimate of θ less than 1.5. On the other hand, an SV of 4.5 for θ, yielded estimates of K less than 200 and estimates of θ between 5 and 10, with each estimate similar across models. But in all cases, CVs of estimates of K and θ were very high, greater than 10, making the estimates uninformative. For the annual censuses, similar dependence on SVs was observed for additive error models, but for multiplicative error both SVs of 1 and 4.5 returned similar estimates of $K > 1000$ and $\theta < 1$. Again CVs were larger than 10. Given that our dataset turned out to be well modelled by exponential growth, the various versions of generalized logistic (CGL, DGL, genRicker, SGL) approximate the exponential with either large values of K or large values of θ; which results in considerable redundancy between K and θ for such data. Statistica, as noted, complained about such redundancy. When estimates were obtained, their CVs indicated these estimates were of no value. Thus, our general conclusion about this data set (exponential growth with no information on K or θ) does not depend on SVs.

RESULTS

Scalar Model Comparisons for Annual (December) Censuses

As for the semi-annual censuses, for the annual census data the discrete-time models exhibited the same deviances so that their ΔAIC_c values differed according to their number (k) of model parameters. Unlike the semi-annual censuses, however, the (naïve) continuous-time models exhibited lower deviances and lower AIC_c values than the discrete-time models. For both error types, the continuous-time exponential model had lowest AIC_c amongst the models in Table 1, though the CGL had lower deviance and in the case of multiplicative error the difference in AIC values between the two continuous-time models was marginal.

Table S1 Results for the comparison of scalar models of Table 1 for the December census data only. Model name abbreviations as in Table 1; R^2 is 1 – (ratio of error sum of squares to total sum of squares) for the regression fit; Dev is the deviance, -2 times the maximized log-likelihood; k is the number of estimable model parameters (including the variance of the residuals); $r \pm$ SE is the estimated value of the parameter r common to all the models as an *annual* rate ± SE; ΔAIC_c is the model's AIC_c value minus that of the model with the smallest AIC_c value, which was the continuous-time exponential (Cexp) for both analyses.

	Additive error					Multiplicative error				
Model	R^2	Dev	k	$r \pm$ SE	ΔAIC_c	R^2	Dev	k	$r \pm$ SE	ΔAIC_c
Cexp	0.995	100.0	2	0.0928 ±0.0033	0	0.996	-57.8	2	0.1005 ±0.0049	0
CGL	0.995	98.8	4	0.0940 ±0.0037	4.5	0.997	-63.1	4	0.123 ±0.029	0.5
Dexp	0.994	105.8	2	0.101 ±0.011	5.8	0.995	-52.2	2	0.104 ±0.016	5.6
DGL	0.994	105.8	4	0.109 ±0.024	11.5	0.995	-52.3	4	0.117 ±0.079	11.3
genRicker	0.994	105.8	4	0.103 ±0.021	11.5	0.995	-52.3	4	0.110 ±0.070	11.3
SGL	0.994	105.8	4	0.103 ±0.021	11.5	0.995	-52.5	4	0.110 ±0.068	11.3

For CGL, the estimate of K was 117 with CV = 0.4 (additive error) and 382 with CV = 2.1 (multiplicative error), while for DGL, genRicker, and SGL about 150 with CV about 6 (additive) and over 1000 with CV about 35 (multiplicative). For CGL, the estimate of θ was

about 16 with CV about 4 (additive error) and 0.7 with CV = 1.6 (multiplicative error), while for DGL, genRicker and SGL about 7.5 with CV about 15.5 (additive error) and 0.8 with CV about 14 (multiplicative error).

For additive error, the deviance of the CGL models with fixed θ decreased (monotonically with increasing θ from $\theta = 1$ to $\theta = 190$) slightly from 99.8 to 99.2 so ΔAIC_c decreased from 2.5 to 1.9. The estimates of K decreased monotonically from 1380 with a CV of 2.2 ($\theta = 1$) to 110 with CV = 0.2 ($\theta = 190$). For multiplicative error, deviance *increased* from -62.9 ($\theta = 1$) to -58.1 ($\theta = 190$) so that ΔAIC_c (relative to the continuous-time exponential) increased from -2.4 to 4.8. Estimates of K followed a similar pattern as for additive error. Thus, the (naïve) continuous-time logistic (i.e., $\theta = 1$ in the CGL) actually gave the best fit to the data for multiplicative error ($\Delta AIC_c = -2.4$ relative to the continuous-time exponential). The estimate of K was 270±100, i.e., CV = 0.37. While this range is biologically plausible, the behaviour of the estimates of K as θ increases indicated that the nonlinear regression was estimating K so that the inflexion point (S2) of the solution lay beyond the observed data. For additive error, increasing θ slightly improved the fit, i.e., these models became more competitive as they better approximated threshold-like models with exponential growth for the actual data, but the opposite was true for multiplicative error, unlike for the semi-annual census data. The fact that the naïve continuous-time models were favoured in the analysis of the annual census data suggests that the stochasticity in the semi-annual census data tended to average out over the annual time step.

For the SGL models with fixed θ, for both error types, deviances and AIC_c values did not vary to any important degree and were not competitive (ΔAIC_c greater than eight for both error types). Estimates of K started unrealistically high with large CVs for $\theta = 1$, decreased monotonically over the rang $\theta = 1$ to 10 to between 150 and 110 with CVs of about 0.7 but for higher values of θ the estimates of K fluctuated outside that range and had extremely large CVs.

Figure S1 shows a plot of the pairs (X_{t-1}, Y_t) for the semi-annual census data, i.e., of the log-transformed census data, modified to account for additions/removals, as the second coordinate (Y_t = ln(ModCount)) versus the log-transformed actual census data at the previous time as the first coordinate (X_{t-1} = ln(PrevCount)), together with the line $y = x + c$, where c is the estimate of (the semi-annual rate) r, from the discrete-time exponential model with multiplicative error, i.e., the overall best fit model. Thus, the line represents this model, viz., $Y_t = X_{t-1} + r + \varepsilon_t$. Figure S2 shows the same plot for the annual census data with c the estimate of (the annual rate) r from the discrete-time exponential model with multiplicative error fit to that data.

Figure S1. The semi-annual census data plotted together with the line $y = x + c$, c = the estimate of r from the discrete-time exponential model with multiplicative error fit to that

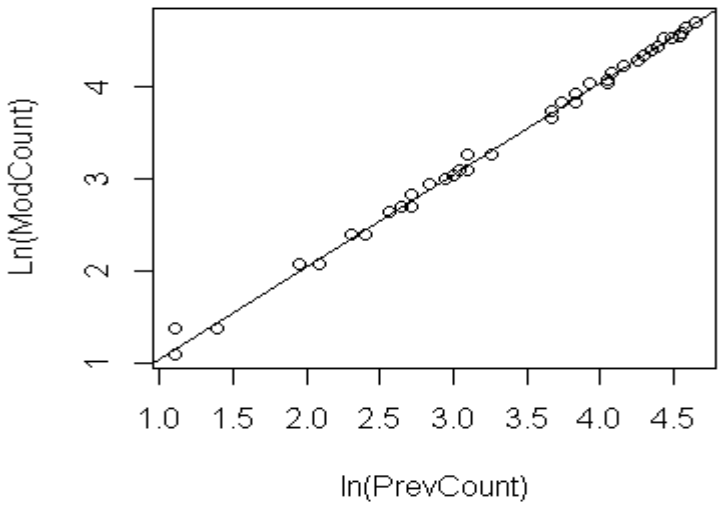

data.

Figure S2. The annual census data plotted together with the line $y = x + c$, c = the estimate of r from the discrete-time exponential model with multiplicative error fit to that data.

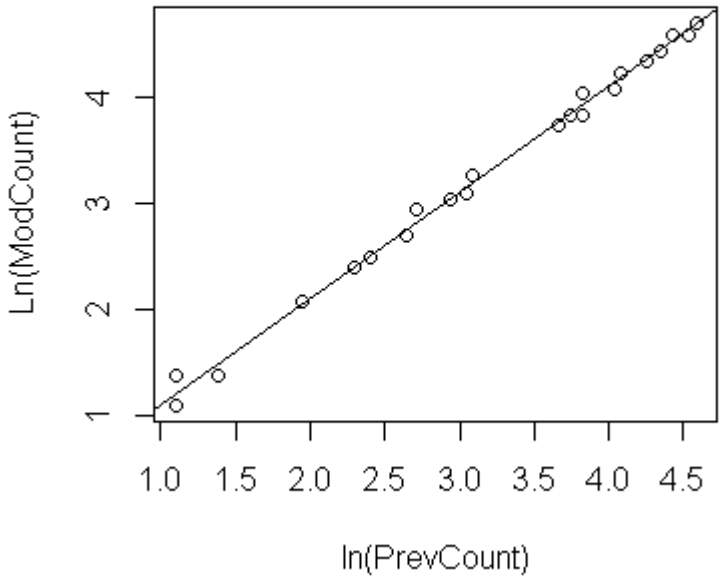

Note that we have not used the jitter option to separate data that coincide, as that would defeat comparison of the fit to the line. In Figure S1, for example, for the first four data (for Dec-86, Jun-87, Dec-87, Jun-88, the Y_t and $X_{t\text{-}1}$ values are equal and so plot as the same point, below the line (at $X_{t\text{-}1} = 1.1$).

Though visual inspection does not quantify the model fit as well as the deviances of the models, note that beyond 3.5 on the horizontal scale in Figure S2, there appears to be a tendency for the data to fall just below the line. It is not just that the June census data has been removed from the plot in Figure S1, but the remaining (December) data is now fit to the exponential model by projecting that data over the larger time step, i.e., whereas Y_t is projected from $X_{t\text{-}1}$ in Figure S1, it is projected from $X_{t\text{-}2}$ (using the same parametrization of censuses as for the semi-annual data) in Figure S2, resulting in the different estimate of r (as an annual rate).

Similarly, the differences between the model fits of the continuous-time exponential and logistic (i.e., $\theta = 1$ in the CGL) and the discrete-time exponential for annual census data and multiplicative error structure appears fairly subtle in a graphical display (Figure S3). The sum of squared residuals for the continuous-time logistic was 0.0733 versus 0.0931 for the continuous-time exponential, the squared residuals of the latter consistently slightly larger than those of the former for years 7 – 17, summing to 137% of the difference in the sum of squared residuals for these two models. Thus, the lower deviance for the continuous-time logistic, which yields a lower AIC_c by 2.4 units, despite the extra model parameter, reflects better model fit for years 7 – 17 rather than indicating a slowing of population growth rate towards the end of the study. The sum of squared residuals of the discrete-time exponential was 0.1200, about 1.6 times larger than that for the continuous-time logistic, which translated into some 8 AIC_c units difference. Thus, there is no evidence that the model fits to the longer time-step are more informative than the fits to the semi-annual census data. That smaller residuals occurred for the fit of a continuous-time model than for a discrete-time model indicated that the annual census data was more easily fit with a projection from an initial value rather than an adjustment each time step, i.e., that the annual census data smoothed out the irregularities in the semi-annual census data.

Dennis et al. (1991) Model

The computation of Dennis et al.'s estimate of their μ from (S8) agreed to nine decimal places with the Statistica estimates of r for the discrete-time exponential model using either semi-annual or annual census data. Agreement of estimates of SEs was less close, to eight decimal places using the annual census data and seven using the semi-annual census data. Agreement for the estimates of σ^2 was to more than 10 decimal places using either set of data. For the annual census dataset, the Dennis et al. model had a lower deviance than any model with additive error, and was also about 7.7 AIC_c units below the (naïve) continuous-time exponential model.

Figure S4 Annual census data, multiplicative error structure. Response variables plotted on the log scale: observed (modified) count (●); predicted responses for the continuous-time exponential (Δ), continuous-time logistic (○), and discrete-time exponential (□).

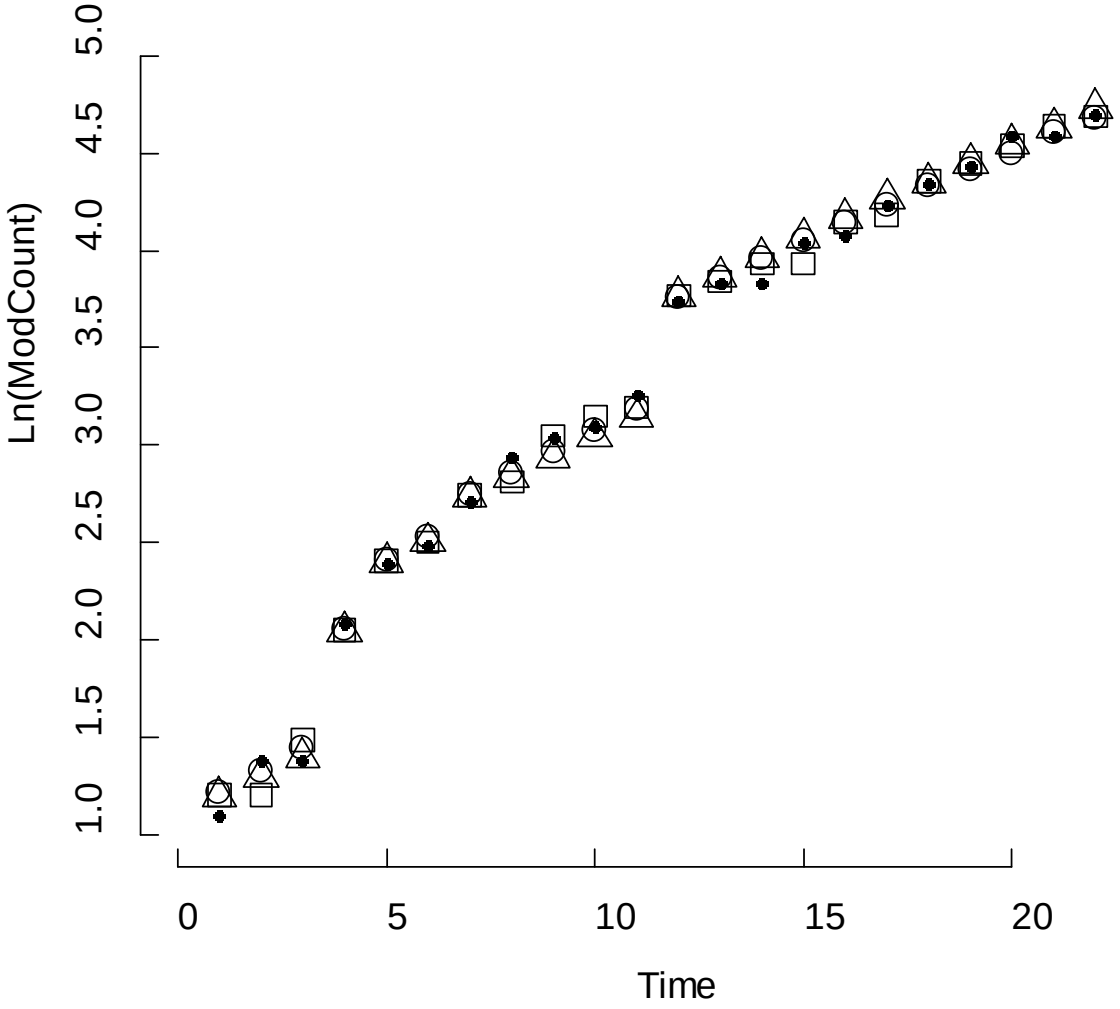

Estimating Demographic and Environmental Stochasticity from the Unstructured Population

Process noise, i.e., departure from the deterministic model, is interpreted as arising from demographic and environmental sources of stochasticity. For a population of statistically identical individuals, Engen *et al*. (1998) provided a decomposition of the variance in the change in population size from a given population size, which provided definitions of demographic and environmental stochasticity and demographic covariance. Sæther *et al*. (1998a) showed how to apply this formalism to demographic data and a time series of abundances (outlined in Lande *et al*. 2003; see also Morris and Doak 2002:127–133).

Environmental stochasticity is typically construed as variations from year to year rather than at finer scales, so we conducted this analysis on an annual basis. For each end-of-year (i.e., our December censuses), 1986 through 2007, we tabulated the contribution each individual alive at that time made to the following end-of-year census: counting one for survival and one for producing an offspring during that year that survived to the end of the year. The usual estimate of variance applied to this annual data defines a quantity $V_d(\mathrm{N})$ for each such end-of-year, which is parametrized by the population size rather than time. As noted above, the formalism assumes that individuals are statistically identical; in particular, for any given year, the individuals alive at that time are assumed to have the same expected contribution to the population the following year. This assumption thus ignores, for example, stage differences such as the difference between immature individuals that contribute only by survival and mature individuals that can also contribute by reproduction. Typically, the formalism is applied to subunits of a population (e.g., females) that can plausibly be treated as homogeneous and to populations in which individuals mature over one time step. Since we are attempting to interpret the process noise of a scalar population model, which also neglects differences between individuals, we proceed as if the formalism is applicable to our data noting that our estimate of $V_d(\mathrm{N})$ conflates strict demographic stochasticity and fixed demographic differences between individuals (such as stage differences), but is still demographic in nature. This conflation may lead to biases in estimates of probability of extinction and time to extinction (Fox and Kendall 2002, Kendall and Fox 2002, Morris and Doak 2002:132–133, Melbourne and Hastings 2008) but our concern is only to estimate the relative demographic and environmental contributions to process noise.

As the best description of the semi-annual data was the discrete-time exponential model, we took that model as the best deterministic model for the SKKR population dynamics and applied it to the December annual census data, i.e., we converted the value of r obtained from the discrete-time exponential model with multiplicative error for the semi-annual census data, to an annual time step. The prescription in Sæther et al. (1998a) (also Lande et al. 2003, equation (1.11); Morris and Doak 2002, equation (4.14)) is to put

$$\left[\frac{N_{t+1}}{N_t} - e^r\right]^2 = \sigma_e^2(N_t) + \frac{V_d(N_t)}{N_t} \qquad \text{(S17)}$$

where N_t is the observed abundance at time t (the December for which one computes the contributions of living individuals to time t+1) and N_{t+1} is the abundance at time t+1. For our data, we must replace N_{t+1} by M_{t+1}, the modified count at t+1 to account for any introductions or removals during the time step (see the section **Including Additions and Removals in Population Modelling** above). Using the estimate of $V_d(N_t)$ obtained as described in the previous paragraph, one obtains from (S17) an estimate $\sigma_e^2(N_t)$ of the environmental contribution to process noise.

The advice (Sæther et al. 1998a, Morris and Doak 2002, Sæther and Engen 2002, Lande et al. 2003) is then to regress each of V_d (N_t) and $\sigma_e^2(N_t)$ on N_t to check for density dependence. For V_d (N_t), regression yielded a slope of -0.00040 (p = 0.55) and with a positive intercept (p = 0.00016), while for $\sigma_e^2(N_t)$, regression yielded $p > 0.2$ for both slope and intercept. The t-test for each set of V_d (N_t) and $\sigma_e^2(N_t)$ values returned p = 0.000001 for the former (mean = 0.137 ± 0.091) and p = 0.44 for the latter. Thus, density dependence was detected for neither V_d (N_t) nor $\sigma_e^2(N_t)$, but the mean of V_d (N_t) is judged to be nonzero. Overall estimates of the demographic and environmental contributions to process noise are obtained as weighted means of V_d (N_t) and $\sigma_e^2(N_t)$ (Sæther and Engen 2002:194, 197), for which we obtained 0.127 and 0.0002, respectively.

Our strategy of including all individuals for the computation of demographic stochasticity is conservative; it is more usual to restrict to the female segment of the population. Doing so returned an estimate of 0.178, in place of 0.127, for σ_d^2, without altering any other conclusions of the previous paragraph other than increasing the component of σ_d^2 due to fecundity to 92%.

Matrix Models

All matrix computations were performed in R 2.15.1(R Development Core Team. 2009. R: A language and environment for statistical computing. R Foundation for Statistical Computing, Vienna, Austria. ISBN 3-900051-07-0, URL http://www.R-project.org).

The projection matrix A for Goodman's model takes the form

$$A = \begin{pmatrix} B & 0 \\ D & Q \end{pmatrix} \qquad \text{(S18)}$$

where the matrix B is the female-only matrix model for the population dynamics, the matrix Q is the analogue for males but encodes only survival as males are not modelled as contributing to reproduction, and the matrix D encodes the production of male offspring by females. The matrix A is reducible (Caswell 2001:90) but, assuming B and Q are irreducible, for a realistic two-sex model, i.e., one in which the stable-stage distribution (SSD) contains both males and females, one can show that the dominant eigenvalue λ_A of A has (right) eigenvector (w_F, w_M) with each of w_F and w_M nonzero and with strictly positive components. Moreover: λ_A is the dominant eigenvalue of B with (right) eigenvector w_F; the left eigenvector of A (i.e., the reproductive value vector when appropriately scaled) is $(v_F, \mathbf{0})$

where v_F is the left eigenvector of λ_A as dominant eigenvalue of *B*; the sensitivities of λ_A with respect to entries of *D* and *Q* are zero and both the sensitivities and elasticities of λ_A with respect to entries of *B* are unambiguous as to whether one considers them as properties of the two-sex or female-only model.

We employed a stage-based rather than age-based model as life stages defined as biological states are more relevant than age (Law and Linklater 2014). For each sex, the biological states of interest are calf (C), subadult (S), and adult (A) (prefixed by F or M to specify sex, e.g., FC for female calf), as defined in the text and Law and Linklater (2014). The nonzero entries of matrix *B* consist of transition rates *G* between stages, survival rates *P* within stages, and fecundity rates *F* for the production of female offspring. The matrix *Q* will have an identical structure except that where the fecundity rates occur in *B* the corresponding entries in *Q* are zero. The only nonzero entries of *D* are for the fecundity rates for the production of male offspring from females. Though the stages C, S, and A are of primary biological interest, for a semi-annual time step we could build a more accurate matrix model for SKKR as regards transition rates by partitioning C and S into substages. For SKKR, calves became subadults beyond 1.5 years of age and subadults became adults beyond 2.5 years of having become a subadult. There were calves of both sexes that did become subadults before the age of two and females that became adults in their third year of being a subadult. As males were not considered adult until age eight, they became adult at least a year later than females became adults.The purpose of the substages was to exclude transitions from the first year as a calf and the first two years as a subadult. The ‘stages’ for the matrix model then were C1a (calf at most 6 months old), C1b (calf, 6 months < age ≤ 12 months), C2 (calf, age > 12 months), S1a (subadult, within 6 months of becoming subadult), S1b (subadult, time since becoming subadult greater than 6 months but less than or equal to 12 months), S2a (subadult, time since becoming subadult greater than 12 months but less than or equal to 18 months), S2b (subadult, time since becoming subadult greater than 18 months but less than or equal to 24 months), S3 (subadult, time since becoming subadult greater than24 months), A (adult), for each sex. So as to retain the term ‘stage’ for the biological states of C, S, A, we refer to these `stages’ as substages. The matrix *B* takes the form

$$B = \begin{pmatrix} 0 & 0 & 0 & 0 & 0 & 0 & 0 & F_S & F_A \\ G_{C1a\to C1b} & 0 & 0 & 0 & 0 & 0 & 0 & 0 & 0 \\ 0 & G_{C1b\to C2} & P_{C2} & 0 & 0 & 0 & 0 & 0 & 0 \\ 0 & 0 & G_{C2\to S1a} & 0 & 0 & 0 & 0 & 0 & 0 \\ 0 & 0 & 0 & G_{S1a\to S1b} & 0 & 0 & 0 & 0 & 0 \\ 0 & 0 & 0 & 0 & G_{S1b\to S2a} & 0 & 0 & 0 & 0 \\ 0 & 0 & 0 & 0 & 0 & G_{S2a\to S2b} & 0 & 0 & 0 \\ 0 & 0 & 0 & 0 & 0 & 0 & G_{S2b\to S3} & P_{S3} & 0 \\ 0 & 0 & 0 & 0 & 0 & 0 & 0 & G_{S3\to A} & P_A \end{pmatrix}$$

(S19)

As noted already, the matrix Q takes the same form except that the F_S and F_A entries are zero, while the matrix D has entries M_S and M_A in the final two columns of its first row (for the production of male offspring) as its only nonzero entries. We parametrized these matrices, i.e., estimated their nonzero entries, in two different ways, yielding two realizations of the matrix model. All matrix-model analyses were performed with both parametrizations as a check on the robustness of results.

For the first parametrization, P's and G's were modelled in terms of probability of transition between stages and survival during stages. For each sex and stage (not substage), we computed the ratio of the number of individuals of that sex that died during that stage to the total time individuals of that sex and stage were at risk (i.e., alive) as an estimate of mortality rate and subtracted this quantity from one to obtain a sex-specific, stage-based survival rate σ (e.g., Brault and Caswell 1993). In this parametrization we did not distinguish survival for substages of a given stage because we regard stage as the state of biological interest and substages as conveniences for model parametrization. For each of C1a → C1b, C1b → C2, S1a → S1b, S1b → S2a, S2a → S2b, S2b → S3, transition is automatic given survival over the time step. Thus, for each sex,

$$G_{C1a\to C1b} = G_{C1b\to C2} = \sigma_C \text{ and } G_{S1a\to S1b} = G_{S1b\to S2a} = G_{S2a\to S2b} = G_{S2b\to S3} = \sigma_S \qquad \text{(S20)}$$

The probabilities of transitions C2 → S1a and S3 → A were estimated as follows. For FC2 → FS1a, we computed the mean duration of calfhood for those females that were born and transitioned from calf to subadult during the study, subtracted 1 year (i.e., two time units) from this mean, and took the reciprocal to define the probability $\gamma_{FC2\to FS1a}$ (Brault and Caswell 1993, Caswell 2001, §6.4.1). For FS3 → A, we computed the mean duration of subadulthood for those females that transitioned from calf to subadult and subadulthood to adulthood during the study, subtracted 2 years (i.e., four time units) from this mean, and took the reciprocal to define the probability $\gamma_{FS\#\to FA}$. Analogous quantities were computed for the transitions MC2 → MS1a and MS3 → MA. Now, suppose there are $n(t)$ individuals in some specific substage (FC2, MC2, FS3, or MS3) at time t. In reality, transitions to the next substage (FS1a, MS1a, FA, MA, respectively) can occur at any time between t and t+1. Let u be an element of [0,1]. If all transitions occur at time t+u, with probability γ, and if σ is the survival rate for the stage that individuals transition from and ς is the survival rate of the stage to which individuals transition to, then

$$\begin{aligned} n(t) &= (1-\sigma^u)n(t) + (1-\varsigma^{1-u})\gamma\sigma^u n(t) + \varsigma^{1-u}\gamma\sigma^u n(t) + \sigma^{1-u}(1-\gamma)\sigma^u n(t) \\ &+ (1-\sigma^{1-u})(1-\gamma)\sigma^u n(t) \end{aligned} \qquad \text{(S21)}$$

i.e., the $n(t)$ can be written as the sum of : those that don't survive until time t+u; those that survive until t+u, transition to the next stage but don't survive until time t+1; those that

survive until $t+u$, transition to the next stage and survive until time $t+1$; those that survive until time $t+u$, don't transition to the next stage and survive until time $t+1$; and those that survive until time $t+u$, don't transition to the next stage and don't survive until time $t+1$.

Hence, the transition rate from the one stage to the next and the persistence rate within the initial stage are, respectively

$$G_u = \varsigma^{1-u}\gamma\sigma^u \qquad P_u = \sigma^{1-u}(1-\gamma)\sigma^u = (1-\gamma)\sigma \qquad \text{(S22).}$$

Taking the mean over u in [0, 1] yields

$$G = \int_0^1 G_u\,du = \int_0^1 \varsigma^{1-u}\gamma\sigma^u\,du = \gamma\varsigma\int_0^1\left(\frac{\sigma}{\varsigma}\right)^u du = \gamma\varsigma\left[\left(\frac{\sigma}{\varsigma}\right)^u\right]_0^1\left[\ln\left(\frac{\sigma}{\varsigma}\right)\right]^{-1} = \frac{\gamma(\sigma-\varsigma)}{\ln\left(\sigma/\varsigma\right)} \qquad \text{(S23)}$$

and

$$P = \int_0^1 P_u\,du = (1-\gamma)\sigma \qquad \text{(S24).}$$

We used formula (S23) for $G_{C2\to S3}$ and $G_{S3\to A}$ and (S24) for $P_{C2\to C2}$, $P_{S3\to S3}$, $P_{A\to A}$, for each sex.

Reproduction takes place either by existing female adults or by female subadults that transition to adulthood by virtue of giving birth. For fecundity F we first computed the fertility (i.e., birth rate) m of adult females as the ratio of the number of births (of a specific sex), excluding births that initiated the transition of the mother from subadulthood to adulthood, to the total number of female-adult time units during the study. We computed the probability α that a female transitioned from subadulthood to adulthood by giving birth (as opposed to reaching the age of seven years without having given birth) as the ratio of number of females that did so transition to the total number of females that transitioned from subadulthood to adulthood during the study. Let φ be the birth sex ratio for females, i.e., F/(M+F), and μ that for males, i.e., M/(M+F). If there are $n_A(t)$ adult females and $n_S(t)$ female subadults at time t, and female adults give birth at time $t+u$, u in [0, 1], the following number of female offspring will survive to time $t+1$,

$$n_A(t)\sigma_{FA}^u m_F \sigma_{FC}^{1-u} \qquad \text{(S25)}$$

(i.e., a female adult must first survive to time $t+u$, then give birth, and then its calf must survive to $t+1$ to be censused at $t+1$; our calculation is an adaptation of Caswell 2001, §6.7.1), while females transitioning from subadulthood to adulthood by giving birth, at time $t+v$, v in [0, 1], will produce

$$n_S(t)\sigma_{FS}^v \gamma_{FS3\to FA}\alpha\phi\sigma_{FC}^{1-v} \qquad \text{(S26)}$$

female offspring that survive to time t+1. We next took the means of u in [0, 1] and v in [0, 1] to obtain the per capita fecundities

$$F_A = m_F \sigma_{FC} \int_0^1 \left[\frac{\sigma_{FA}}{\sigma_{FC}} \right]^u du = \frac{m_F (\sigma_{FA} - \sigma_{FC})}{\ln\left(\sigma_{FA} / \sigma_{FC} \right)} \qquad \text{(S27)}$$

$$F_S = \gamma_{FS3 \to FA} \alpha \phi \sigma_{FC} \int_0^1 \left[\frac{\sigma_{FS}}{\sigma_{FC}} \right]^v dv = \gamma_{FS3 \to FA} \alpha \varphi \frac{\sigma_{FS} - \sigma_{FC}}{\ln\left(\sigma_{FS} / \sigma_{FC} \right)} \qquad \text{(S28).}$$

Replacing m_F by m_M, σ_{FC} by σ_{MC}, and φ by μ, yields the fecundities for male offspring production that give the two nonzero entries for matrix D.

The description of our first parametrization (MM1) of the matrix model is now complete. The second parametrization was based on Caswell (2001, §6.1.1). The population projection matrix A can be written as the sum T+F, where the matrix T describes transitions and the matrix F describes reproduction (Caswell 2001:110). Since each individual's state is known throughout the study period, one can estimate T as follows. Namely, for each t, one records the number m_{ij} of individuals in (sub)stage j at time t that end up in (sub)stage i at time t+1, where 'death' is a possible fate. The matrix $M_t = (m_{ij})$ contains the matrix T_t as its first s rows, where s is the number of (sub)stages; its final row contains the mortality information. Caswell (2001, §6.1.1) recommends summing the M_t over t to obtain a matrix M, and then taking the transition probability p_{ij} from stage j to stage i to be the ij'th entry of M divided by the sum over rows of the entries of j'th column of M (this estimate is motivated by maximum likelihood estimation). This approach computes P's and G's directly rather than σ's and γ's. We computed the fecundities using the formulae (S25–S28) modified so that the transition rates computed in the current method replaced transition and survival rates as computed for the MM1 parametrization. In particular, for σ_{FS} we used the sum of the transition rates FS3 → FS3 and FS3 → FA, for σ_{FC} the transition rate FC1a → FC1b, for σ_{MC} the transition rate MC1a →MC1b, and for σ_{FA} the transition rate FA → FA. The description of the second parametrization (MM2) is now complete. The actual parametrizations are recorded in Tables S3 and S4. The most notable difference between MM1 and MM2 is that, for MM2, individuals were more likely to remain within the substage C2 or S3 rather than transition to the next stage, with the consequence that the fecundity F_S was lower for MM2 and individuals reached the adult stage at a slower rate, for both sexes.

Table S2 The survival and fertility parameters for the SKKR population. Birth sex ratio is F/(M+F) for females and M/(M+F) for males, where F = number of female births, M = number of male births. The quantity α is the probability that a female transitioned from subadulthood to adulthood by giving birth rather than having reached the age of seven years without having given birth.

Parameter	Female	Male
σ_C	0.9977	0.9977
σ_S	0.9820	0.9841
σ_A	0.9959	0.9892
$\gamma_{C2\rightarrow S1a}$	0.3704	0.3529
$\gamma_{S3\rightarrow A}$	0.2578	0.1604
Birth sex ratio	0.5619	0.4381
m (fertility)	0.1029	0.0797
α	0.6207	

Table S3 Nonzero entries of the two matrix models MM1 and MM2. The entries in the 'female' column yield the female-only part of the model (i.e., the matrix *B*, (S19)), the entries in the 'male' columns for fecundities F_{S3} and F_A are the nonzero entries of the matrix *D* and the remaining entries in the 'male' columns given the nonzero entries for the matrix *Q* , in (S18).

	MM1		MM2	
Entry	female	male	female	male
$G_{C1a\to C1b}$	0.9977	0.9977	0.9897	0.9899
$G_{C1b\to C2}$	0.9977	0.9977	1	1
$G_{C2\to S1a}$	0.3666	0.3497	0.3409	0.3173
$G_{S1a\to S1b}$	0.9820	0.9841	1	0.9
$G_{S1b\to S2a}$	0.9820	0.9841	0.9773	1
$G_{S2a\to S2b}$	0.9820	0.9841	0.9762	0.9583
$G_{S2b\to S3}$	0.9820	0.9841	0.9487	1
$G_{S3\to A}$	0.2549	0.1583	0.2243	0.1087
P_{C2}	0.6282	0.6456	0.6591	0.6827
P_{S3}	0.7289	0.8262	0.7664	0.8913
P_A	0.9959	0.9892	0.9958	0.9878
F_S	0.0890	0.0694	0.0775	0.0604
F_A	0.1025	0.0795	0.1021	0.0792

A useful measure of the difference between two population vectors is Keyfitz's Δ (e.g., Caswell 2001:101). For any two population vectors *X* and *Y*, convert each to a vector of proportions by dividing each component by the sum of that vector's components. If the resulting vectors of proportions (which sum to one for each vector) are *x* and *y*, then

$$\Delta(X,Y)=\frac{1}{2}\sum_i |x_i - y_i| . \qquad \text{(S29)}$$

Keyfitz's Δ has a maximum value of one and is zero when the two vectors coincide.

To compare the projections of the two parametrizations, we collapsed the projections of MM1 and MM2 into stage-based population vectors and then computed Keyfitz's Δ for the two projections for each semi-annual census date Jun-99 through Dec-08. Δ = 0.008 in Jun-99, increased monotonically to 0.028 in Dec-00, then decreased monotonically to 0.024 in Dec-03, remained at that value through Dec-05, increased to 0.025 for Jun-06 through Jun-07, and then returned to 0.024 for Dec-07 through Dec-08, with mean 0.0241 and SD 0.0043. Thus, the overall difference between the projections of the two parametrizations is small.

Our primary interest in the matrix model was in modelling the dynamics of the stage-structured population after introductions ceased, from Dec-98 through Dec-08. The SKKR population was still a young population. In particular, no rhinoceros born in GFFR died of old age during the study. Thus, though matrix entries of MM1 and MM2 might be plausibly considered representative of the dynamics during the study, as adults age, and deaths due to old age become common, the survival rate of adults will decrease below that during the study period. Thus, the asymptotic dynamics of the matrix model should not be confused with the asymptotic dynamics of the actual population, even in the absence of density dependence in the actual population. Thus, the asymptotic dynamics of the two parametrizations are only indicative of the model and of how the population might have been expected to behave in the long term had nothing else changed, which as noted is unrealistic. The asymptotic properties of the matrix model then are of interest as indicators of how well the matrix model describes an exponentially growing population of large herbivores ('slow' mammals) with adult survival rates that are somewhat too high in the long run (e.g., Brodie et al. 2011 estimated adult female survival as 0.944, 95% CI = 0.920 – 0.962 and adult male survival as somewhat lower but larger than 0.9).

Although the matrix models were constructed on a semi-annual time step and with substages for accuracy, our interest is in the biological states C, S, A. Hence, after analyses, substages were collapsed to stages for the purposes of comparison and all comparisons were made on an annual basis. The annual intrinsic rate of increase r was 0.1024 (MM1) or 0.0994 (MM2). MM1 and MM2 had the same overall patterns for their 18 eigenvalues and eigenvectors. In order of decreasing magnitude, after the dominant eigenvalue, 1.0525 (MM1) or 1.0510 (MM2), the next two eigenvalues were both real with ratios of 0.99 (MM1 and MM2) and 0.83 (MM1) or 0.89 (MM2) to the dominant. For both parametrizations, the eigenvectors of these two eigenvalues had nonzero components only for the MA, and for the MS3 and MA, components, respectively. The significance of these facts is that the approach to the stable stage distribution (SSD) of the matrix models will be slowest for these two components, i.e., for male adults and MS3s. There follows a complex conjugate pair of eigenvalues, two further distinct real eigenvalues, and two distinct pairs of complex conjugate pairs. Each of these eigenvalues has a single eigenvector. The final eigenvalue (real) has a single linearly independent eigenvector of multiplicity six. The second, third, seventh and last eigenvalues are all real and are the eigenvalues of the matrix Q; the fact that the last eigenvalue has algebraic multiplicity six but only geometric multiplicity one reflects the fact that the matrix Q is singular. The other eigenvalues are those of the female-only matrix model

B. The elasticity of λ with respect to adult female survival was the largest elasticity, 0.5396 (MM1) or 0.5349 (MM2), all other elasticities were less than 0.1, and ordered by magnitude in the same way for the two models, with the least being that with respect to the fecundity F_S, 0.0059 (MM1) or 0.0055 (MM2). In decreasing order of magnitude, after the highest elasticity comes that with respect to FS3 survival, then that with respect to FC2 survival, then that with respect to each of the transitions FC1a → FC1b, FC1b →FC2, FC2 → FS1a, FS1a → FS1b, FS1b → FS2a, FS2a → FS2b, FS2b → FS3 all of which coincide, then that with respect to the transition FS3 → FA and that with respect to the fecundity F_A, which coincide, and finally the smallest, that with respect to the fecundity F_S (see Table S8 for values). The reproductive values of the substages increased from a (normalized) value of 1 for FC1a to a value of 1.81 (MM1) or 1.85 (MM2) for FA (recall that male (sub)stages have zero reproductive value for the Goodman two-sex model). Thus, as expected for a long-lived species, the adult female stage has the greatest influence on demography both as regards the influence of adult female survival on λ and reproductive value. As already noted, however, our matrix model does not describe the true asymptotic state of the SKKR population so the elasticity results should not be over interpreted. The stable stage distributions for *stages*, rather than *substages*, are recorded in Table S4, the differences consistent with the previous observation that individuals are slightly more likely to remain as calves or subadults rather than transition to the next stage for MM2 relative to MM1.

Table S4 The stable stage distributions (SSD) for MM1 and MM2.

	MM1	MM2
stage	SSD	SSD
FC	0.1371	0.1395
FS	0.1550	0.1602
FA	0.2826	0.2787
MC	0.1089	0.1122
MS	0.1413	0.1553
MA	0.1751	0.1541

Very roughly, given black rhino reproductive behaviour, one expects a typical adult female black rhino to be accompanied by a calf, and to have one prior calf as a SA in the population (for SKKR, mean (± SD) female calf duration was 2.06 ± 0.80 years; mean male calf duration was 2.05 ± 0.83 years; mean female SA duration was 2.7 ± 1.3 years; mean male subadult duration was 3.1 ± 2.0 years). If the birth sex ratio (BSR) is 1:1, then one

expects the SSD to be roughly (0.5, 0.5, 1, 0.5, 0.5, x) (assuming the SSD is achieved prior to density dependence sets in), where $x < 1$ if adult males survive at a lower rate than adult females. Hence, upon normalizing, one gets a SSD of roughly (0.125, 0.125, 0.25, 0.125, 0.125, y), where $y \leq 0.25$, except that all the figures (i.e., other than *y*) should be a little larger than stated if $x < 1$ ($y < 0.25$), and the figure for MS should be a little larger still and that for MA a little smaller as males are subadults longer, on average, than females are, while the proportion for calves should be slightly less to reflect less than perfect reproduction. Large departures from this rough SSD should reflect departures in the BSR from 1:1. For the SKKR population, which produced 48 F to 38 M during 1999 – 2008, the proportions should be a little higher for females than males (comparing calves with calves, SAs with SAs; (48/38) x 0.125 ≈ 0.158 and (38/48) x 0.125 ≈ 0.099). The SSDs derived from the matrix models are consistent with these expectations. Of course, the onset of density dependence would be expected to alter the proportions of stages.

For each matrix model, the projections approached their SSDs over the period Jun-99 through Dec-08, with Keyfitz's Δ between the projection and the SSD strictly decreasing from 0.227 (MM1) or 0.208 (MM2) to 0.001 (MM1) or 0.004 (MM2), respectively. Thus, the transient behaviour present in the matrix model projections during the period of interest basically consisted of the 'smooth' extinguishing of the deviation from SSD present in the initial population vector (i.e., SKKR in Dec-98). In particular, for the MM1 parametrization, the damping ratios (Caswell 2001, §4.7.1) for the second and third largest eigenvalues were 1.06 and 1.27, respectively, so that exponential damping of their eigenvectors had half-lives of 11.2 and 2.9 years, respectively. Thus, though the proportion of adult males is somewhat slow to approach the SSD proportion (the eigenvector of the second largest eigenvalue has male adults as its only nonzero component), all other eigenvectors are damped fairly rapidly, implying that all other (sub)stages approach their SSD proportions fairly rapidly. For MM2, the half-life for the second largest eigenvalue is the same as for MM1 but that for the third largest eigenvalue is 4.2, slightly larger, implying that MS3 approaches its SSD proportion a little slower than for MM1, as noted previously. All these half-lives, however, are just a fraction of black rhinoceros lifespan.

The five rhinoceros removed from SKKR in May-06 belonged, as of Jun-06, to the following substages: one to each of FS2a, FS2b, MS3, and two to FS3. The corresponding substage population vector was projected forward from Jun-06 by each of MM1 and MM2 and, for Dec-06, Dec-07, and Dec-08, the projected quantities rounded to integers so as to obtain biologically sensible projections (moreover, since the exported male did not turn eight years old until 2009 it was retained as a subadult throughout), resulting in the following stage-based population vectors (FC, FS, FA, MC, MS, MA):

$$\begin{pmatrix}0\\4\\0\\0\\1\\0\end{pmatrix} \qquad \begin{pmatrix}1\\2\\2\\1\\1\\0\end{pmatrix} \qquad \begin{pmatrix}2\\1\\3\\1\\1\\0\end{pmatrix} \tag{S30}$$

for Dec-06, Dec-07, and Dec-08, respectively, for both MM1 and MM2. The final vector for Dec-08 was slightly ambiguous for the MM2 projection, as an alternative interpretation was that the population vector for Dec-08 was the same as that for Dec-07, but we chose the option in (S30) as a consensus result and in order to have a parametrization-independent result. These three vectors were added to the observed SKKR population vectors for Dec-06, Dec-07, and Dec-08. The resulting augmented population vectors, together with the observed SKKR population vectors for each December from 1998 through 2005, were then taken as the actual population vectors to which the matrix projections would be compared. Thus, the actual SKKR substage population vector for Dec-98 was projected semi-annually by each of MM1 and MM2 up to Dec-08. For each December, 1999 through 2008, these projections were collapsed to stage-based population vectors and compared to the actual stage-based population vectors. In addition the projected number of additions per year (i.e., born during that year and survived to the end of that year), by sex, were recorded and compared to the actual number of additions, by sex, per year. In addition to direct comparison, we computed Keyfitz's Δ. The results for both parametrizations are presented in Table S5. Figure S4 shows a plot of various Keyfitz distances.

Figure S4 Keyfitz's Δ for the SKKR population vector and: the SSD of MM1 (solid circles); the SSD for MM2 (open crcles); the projections of MM1 (solid squares); the projections of MM2 (open squares).

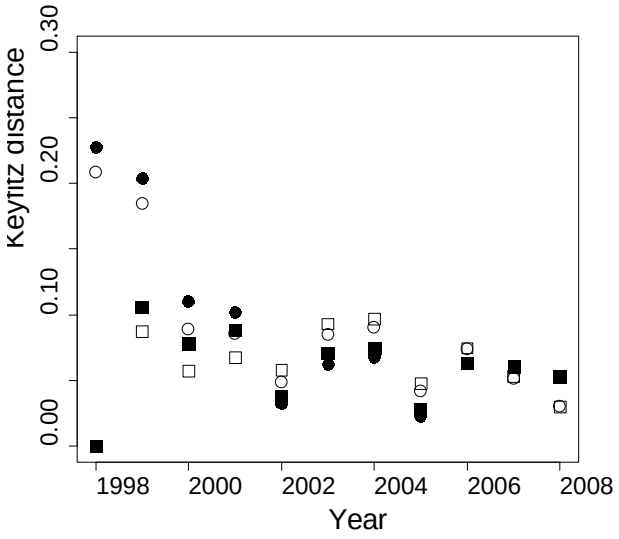

Unlike the projections' monotone convergence on their SSDs, the SKKR population vectors though eventually close to SSDs and model projections exhibited mild fluctuations relative to them.

Table S5 The second and fourth columns list the matrix model projections for the end of year for parametrizations MM1 and MM2, respectively; the third column lists the SKKR population vectors (augmented by the exports of 2006 plus their projections for 2007 and 2008) at the end of year; all these population vectors are formatted as the transpose of the row vector (FC, FS, FA, MC, MS, MA); column six lists the number of female and male recruits each year (augmented by the projected additions from the 2006 exports) as a column vector $\begin{pmatrix} F \\ M \end{pmatrix}$; the fifth and seventh columns list the number of projected female and male recruits each year (recruits are offspring of the year surviving to the end of the year), in the same format as column six, for MM1 and MM2, respectively; the final column lists Keyfitz's Δ for the SKKR population vector of column three and the MM1 Projection in column two (Δ_1), and the MM2 projection in column four (Δ_2) (also plotted in Fig. S5).

Year	MM1 Pop Vec	SKKR Pop Vec	MM2 Pop Vec	MM1 recruits	SKKR recruits	MM2 births	Δ_1 Δ_2
1999	$\begin{pmatrix} 5.6 \\ 9.4 \\ 11.6 \\ 5.0 \\ 9.4 \\ 5.5 \end{pmatrix}$	$\begin{pmatrix} 6 \\ 13 \\ 9 \\ 3 \\ 10 \\ 5 \end{pmatrix}$	$\begin{pmatrix} 5.6 \\ 9.6 \\ 11.2 \\ 4.9 \\ 9.9 \\ 5.0 \end{pmatrix}$	$\begin{pmatrix} 3.1 \\ 2.4 \end{pmatrix}$	$\begin{pmatrix} 4 \\ 0 \end{pmatrix}$	$\begin{pmatrix} 2.9 \\ 2.2 \end{pmatrix}$	0.1059 0.0870
2000	$\begin{pmatrix} 7.2 \\ 8.0 \\ 14.6 \\ 5.9 \\ 9.1 \\ 7.3 \end{pmatrix}$	$\begin{pmatrix} 7 \\ 9 \\ 12 \\ 3 \\ 9 \\ 6 \end{pmatrix}$	$\begin{pmatrix} 7.0 \\ 8.5 \\ 14.0 \\ 5.8 \\ 9.9 \\ 6.4 \end{pmatrix}$	$\begin{pmatrix} 3.6 \\ 2.8 \end{pmatrix}$	$\begin{pmatrix} 1 \\ 0 \end{pmatrix}$	$\begin{pmatrix} 3.4 \\ 2.7 \end{pmatrix}$	0.0774 0.0570
2001	$\begin{pmatrix} 8.1 \\ 8.5 \\ 16.4 \\ 6.5 \\ 9.1 \\ 9.1 \end{pmatrix}$	$\begin{pmatrix} 6 \\ 9 \\ 17 \\ 7 \\ 12 \\ 6 \end{pmatrix}$	$\begin{pmatrix} 8.0 \\ 8.8 \\ 15.8 \\ 6.5 \\ 10.1 \\ 7.9 \end{pmatrix}$	$\begin{pmatrix} 3.7 \\ 2.9 \end{pmatrix}$	$\begin{pmatrix} 4 \\ 7 \end{pmatrix}$	$\begin{pmatrix} 3.6 \\ 2.8 \end{pmatrix}$	0.0879 0.0675

2002	$\begin{pmatrix} 8.9 \\ 9.6 \\ 18.2 \\ 7.1 \\ 9.8 \\ 10.5 \end{pmatrix}$	$\begin{pmatrix} 7 \\ 9 \\ 18 \\ 7 \\ 8 \\ 10 \end{pmatrix}$	$\begin{pmatrix} 8.9 \\ 9.7 \\ 17.6 \\ 7.2 \\ 10.8 \\ 9.1 \end{pmatrix}$	$\begin{pmatrix} 4.1 \\ 3.2 \end{pmatrix}$	$\begin{pmatrix} 3 \\ 0 \end{pmatrix}$	$\begin{pmatrix} 4.0 \\ 3.1 \end{pmatrix}$	0.0372 0.0579
2003	$\begin{pmatrix} 9.7 \\ 10.9 \\ 20.0 \\ 7.8 \\ 10.6 \\ 11.9 \end{pmatrix}$	$\begin{pmatrix} 12 \\ 10 \\ 20 \\ 7 \\ 7 \\ 14 \end{pmatrix}$	$\begin{pmatrix} 9.7 \\ 10.9 \\ 19.3 \\ 7.8 \\ 11.7 \\ 10.4 \end{pmatrix}$	$\begin{pmatrix} 4.5 \\ 3.5 \end{pmatrix}$	$\begin{pmatrix} 7 \\ 4 \end{pmatrix}$	$\begin{pmatrix} 4.3 \\ 3.3 \end{pmatrix}$	0.0703 0.0929
2004	$\begin{pmatrix} 10.7 \\ 12.2 \\ 22.0 \\ 8.5 \\ 11.6 \\ 13.4 \end{pmatrix}$	$\begin{pmatrix} 13 \\ 11 \\ 23 \\ 7 \\ 8 \\ 15 \end{pmatrix}$	$\begin{pmatrix} 10.7 \\ 12.2 \\ 21.2 \\ 8.6 \\ 12.7 \\ 11.7 \end{pmatrix}$	$\begin{pmatrix} 5.0 \\ 3.9 \end{pmatrix}$	$\begin{pmatrix} 5 \\ 3 \end{pmatrix}$	$\begin{pmatrix} 4.7 \\ 3.7 \end{pmatrix}$	0.0743 0.0967
2005	$\begin{pmatrix} 11.8 \\ 13.5 \\ 24.4 \\ 9.4 \\ 12.7 \\ 15.0 \end{pmatrix}$	$\begin{pmatrix} 12 \\ 13 \\ 24 \\ 10 \\ 10 \\ 15 \end{pmatrix}$	$\begin{pmatrix} 11.7 \\ 13.5 \\ 23.4 \\ 9.4 \\ 13.8 \\ 13.0 \end{pmatrix}$	$\begin{pmatrix} 5.5 \\ 4.3 \end{pmatrix}$	$\begin{pmatrix} 4 \\ 6 \end{pmatrix}$	$\begin{pmatrix} 5.2 \\ 4.1 \end{pmatrix}$	0.0276 0.0475
2006	$\begin{pmatrix} 13.1 \\ 14.9 \\ 27.1 \\ 10.4 \\ 13.8 \\ 16.7 \end{pmatrix}$	$\begin{pmatrix} 12 \\ 18 \\ 27 \\ 14 \\ 10 \\ 17 \end{pmatrix}$	$\begin{pmatrix} 13.0 \\ 14.9 \\ 25.9 \\ 10.4 \\ 15.0 \\ 14.5 \end{pmatrix}$	$\begin{pmatrix} 6.1 \\ 4.8 \end{pmatrix}$	$\begin{pmatrix} 8 \\ 7 \end{pmatrix}$	$\begin{pmatrix} 5.8 \\ 4.5 \end{pmatrix}$	0.0628 0.0744

2007	$\begin{pmatrix}14.6\\16.5\\30.0\\11.6\\15.2\\18.6\end{pmatrix}$	$\begin{pmatrix}12\\18\\29\\16\\14\\16\end{pmatrix}$	$\begin{pmatrix}14.3\\16.5\\28.6\\11.5\\16.4\\16.1\end{pmatrix}$	$\begin{pmatrix}6.8\\5.3\end{pmatrix}$	$\begin{pmatrix}3\\6\end{pmatrix}$	$\begin{pmatrix}6.4\\5.0\end{pmatrix}$	0.0604 0.0532
2008	$\begin{pmatrix}16.2\\18.2\\33.3\\12.8\\16.8\\20.7\end{pmatrix}$	$\begin{pmatrix}16\\20\\32\\14\\20\\16\end{pmatrix}$	$\begin{pmatrix}15.8\\18.2\\31.6\\12.7\\18.0\\17.9\end{pmatrix}$	$\begin{pmatrix}7.5\\5.9\end{pmatrix}$	$\begin{pmatrix}9\\5\end{pmatrix}$	$\begin{pmatrix}7.1\\5.5\end{pmatrix}$	0.0522 0.0296

We offer the following account of the results recorded in Table S5. In this account, stages such as FC will refer to the SKKR population vector in comparison to the projections. 'Recruits' are offspring of the year that survive to the end of the year; for the SKKR population, probability of death in the first year after birth was negligible, so recruits are essentially births. First note that while transitions from MS3 to MA occurred in SKKR by a male reaching age eight, in the model they occurred by probability and the matrix model does not capture the actual distribution of male ages in stage S3 of the SKKR population. In 1999, FS was high and FA low compared to the projection, so FS transitioned to FA less than expected by the models while MC was low due to absence of male recruits in 1999; this state of affairs persisted for 2000. The low number of recruits in 2000 combined with the high number of males born in 2001 resulted in FC lagging behind projections but MC having caught up; FS to FA transitions resulted in rough agreement for these stages but MS has grew larger than projected, resulting in a deficit for MA. During 2002, MS to MA transitions brought closer agreement with projections and the remaining stages maintained their status. The high number of female recruits in 2003 put FC ahead of projections but MS began to lag behind projections, reflecting the absence of male recruits in 1999–2000. MA moved ahead of projections indicating a higher transition rate of MS to MA than projected in 2003. In 2004, little had changed except that male recruits are slightly less than projected. In 2005 there was close agreement between projections and SKKR, except that MS still lagged. The discrepancy in FC from 2003 – 2004 has been eliminated. A high number of recruits occurred in 2006 compared to projections; by the end of that year FC lagged by one behind projection, and FS moved ahead of projections (a higher rate of FC to FS transitions than projected, induced by the higher number of actual recruits therefore causing more calves to become independent) but MC was ahead of projections while MS still lagged. The lag in MS 2002 –

2006 appears to reflect the absence of male recruits in 1999 – 2000, the fact that MS deaths, although few, were concentrated in 2003 – 2005 (whereas FS deaths were more spread out over time), and the higher rate of MS to MA transitions noted for 2003. In 2007, FC lagged further behind projection due to the lower number of female recruits than projected, FS was more in line with projections, and the state of affairs for the other stages was basically unchanged. In 2008, a higher number of female recruits than projected occurred, and FC was now in line with projections, while FS had slightly increased its advance over projection since 2007, the excess deriving from the greater-than-projected number of female recruits in 2006. The higher number of male recruits than projected for 2005 – 2007 maintained MC ahead of projections and also pushed MS ahead of projections, but these male recruits had not yet affected MA.

In summary, we propose that the differences in number and sex between the actual annual recruits and the projected recruits and the resulting knock-on effects as calves transition to subadults and subadults to adults appear to explain much of the discrepancy between the SKKR population vectors and matrix-model projections. The fluctuations in Keyfitz's Δ, both between the SKKR population vectors and the projections and between the former and the SSD (Fig. S4), are greater than the transient behaviour manifest in the matrix models themselves for the period 98 – 08 (Fig. 1). Nevertheless, as measured by Keyfitz's Δ, the differences between the actual SKKR population vectors and the matrix model projections is small, less than 0.1 after 1999.

Transient Dynamics

We noted that the asymptotic properties of the matrix model are of limited interest as the SKKR population was still young and adult mortality rates will increase after 2008 due to individuals dying of old age and eventually density dependence will have some effect also. The primary interest then of the asymptotic properties of the matrix model was in assessing closeness of the matrix model projections during 98–08 to the SSD as an indication of transient dynamics (Fig. 1). Koons *et al*. (2005) drew attention to the fact that sensitivities of transient growth may differ from sensitivities of asymptotic growth. The period Dec-98 through Dec-08 is of interest not only for understanding transient dynamics in their own right but also because during this period removals commenced to source reintroductions elsewhere, so any transient behaviour may have consequences for such harvesting.

We used the matrix model (we conducted the following analyses for each parametrization MM1 and MM2; results were very similar and we only report those for MM1) to project the SKKR substage population vector for each December, 1998 through 2007, through two time steps to the following December, compared that projection with the SKKR population vector for the December to which the projection was made using Keyfitz Δ applied to the stage-based population vectors (i.e., after collapsing substages), and computed the transient annual growth rate for each such projection as

$$GR = \frac{e' A^2 n}{e' n} \qquad \text{(S31)}$$

where n is the SKKR substage population vector , e is a column vector all of whose components are 1, and e' denotes its transpose. Note that for this computation, the SKKR vectors did not need to be augmented with the exports and their projections to 2007 – 2008, except that the exports themselves were retained for the SKKR 2006 population vector that was compared to the projection from the 2005 SKKR population vector. The exports were excluded from the 2006 SKKR population vector that was projected to 2007. For the 10 projections, the mean GR ± SD was 1.1111 ± 0.0084 as compared to the asymptotic *annual* growth rate (λ) of 1.1078 of MM1, and individual values differed from the asymptotic rate by less than 1.8% of the asymptotic rate (Table S6). These results are consistent with the fact (Fig. S4) that SKKR population vectors during this period did not stray much from the SSD.

Table S6 Transient annual growth rates computed from (S31) from actual SKKR substage population vectors, each December, 1998–2007.

Year	Growth rate
1998	1.1078
1999	1.1191
2000	1.1267
2001	1.1127
2002	1.1140
2003	1.1166
2004	1.1118
2005	1.1030
2006	1.0967
2007	1.1026

Values of GR below λ could sound a warning to managers planning to remove animals during the coming year that the population vector is currently expected to perform below the stable rate λ. For SKKR, that condition pertained from 2005–2007, with values smaller by -0.4, -1.0, and -0.5% of the value of λ, respectively. The smallest value for GR

occurred for the projection from Dec-06 to Dec-07, after the removals of the five SAs. These five were expected to have contributed two new animals to the population during that year according to equation (S30), which might account for that lowest anticipated annual recruitment from 2006 to 2007.

Keyfitz's Δ between the projection to a given December and that December's SKKR population vector (after collapsing substages) averaged 0.054, with a SD of 0.025 and a low of 0.020 for the projection from 2003 to 2004 (Fig. S5). These values allow a retrospective assessment of actual population performance versus anticipated performance based on the matrix model. For example, note that the largest value of *GR* occurred for the projection from Dec-00 to Dec-01, which is also the projection for which the disparity between actual and predicted performance is greatest as measured by Δ. During that year, there were 11 animals recruited to the population but the projected number was only about three, so the SKKR population actually outperformed the annual projection that year. The lowest value of Δ occurred for the projection Dec-03 to Dec-04, for which *GR* had its third highest value; for this year actual additions (eight) and anticipated additions coincided closely. For the three years in which *GR* was less than λ, Δ was never large than 0.05 so actual population performance was similar to predictions. Further years of data would have been interesting to see if there was a signal of a trend in these values of *GR* less than λ.

Figure S5 Plot of Keyfitz's Δ between the projections over one year (two time steps) of matrix model MM1 of SKKR population vectors for each December, 1998–2007, and the actual SKKR population vector the following December.

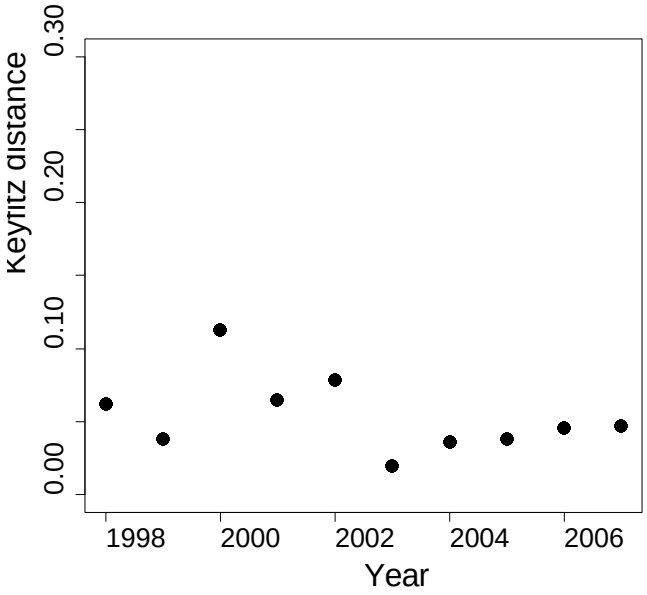

In Fig. S6, the SKKR population vectors exhibit the least convergence on MM1's SSD, MM1's projections from Dec-98 the most, with the annual projections reflecting the proportions of the SKKR vector of the previous year. As argued on pp. 29–30, it is the discrepancies in actual recruits from projected recruits, manifest in the fluctuations of the proportions of calf stages that result in the deviation of the actual population dynamics from those of the model.

Figure S6 The proportion of each stage-and-sex, is plotted against year, Dec-99 through Dec-08 for: the matrix model (MM1) stable stage distribution (●); the SKKR population vector (Δ); the matrix model (MM1) projections of the SKKR population vector in Dec-98 (□); and the matrix model projection (MM1) of the SKKR population vector from the previous December to that year's December (○). The SKKR population vector in Dec-98 was (FC,FS,FA,MC,MS,MA) = (5,11,8,3,11,4) with proportions (0.12,0.26,0.19,0.07,0.26,0.10) versus the SSD of (0.14,0.155,0.28,0.11,0.14,0.175).

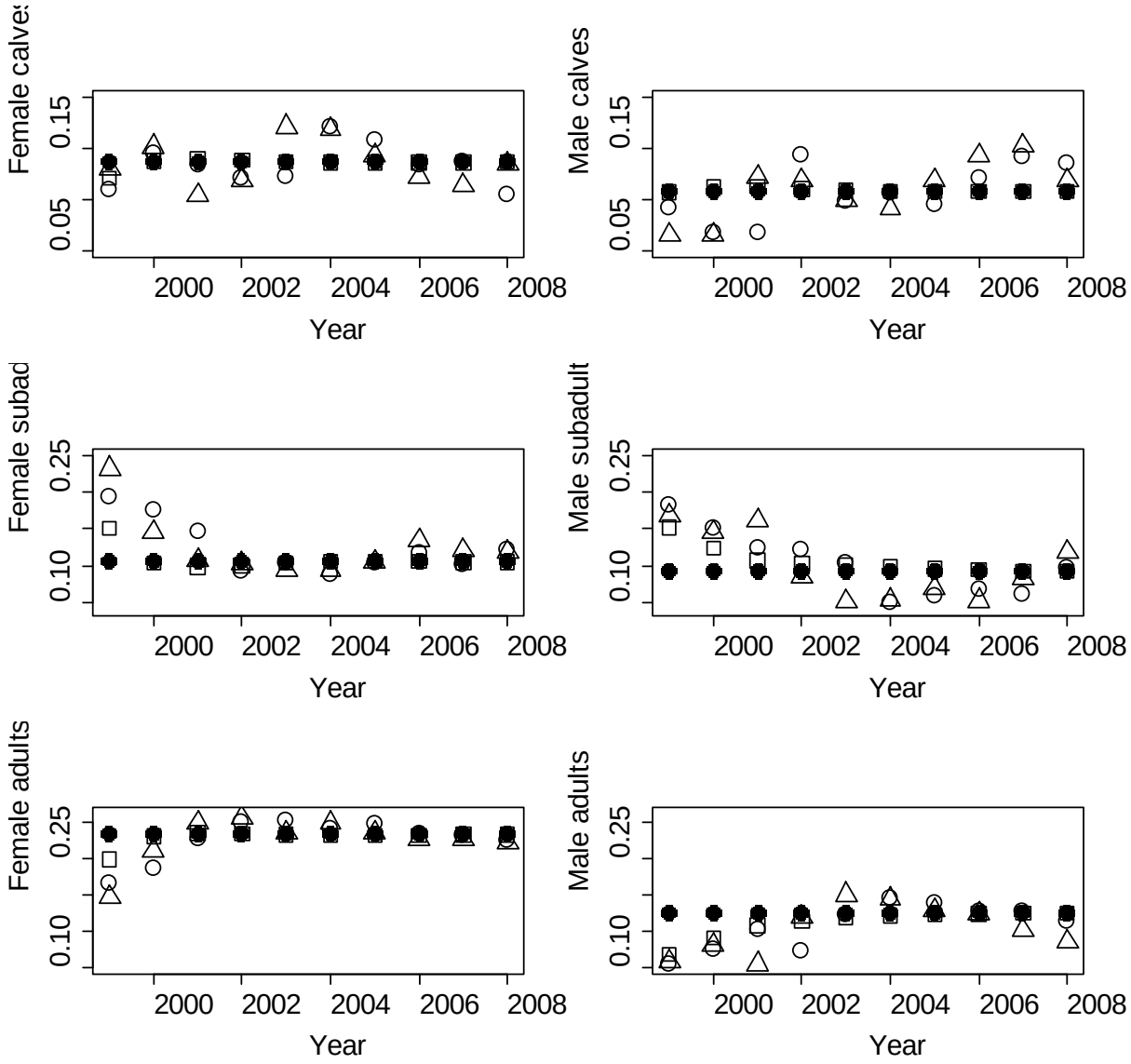

Koons *et al*. (2005) computed the sensitivities to entries a_{ij} of A of the growth over a single time step at arbitrary time t-1

$$GR_t = \frac{e' A^t v}{e' A^{t-1} v}, \qquad \text{(S32)}$$

where v is the population vector at time t-1 , by calculating the partial derivatives of GR_t to a_{ij}. As an aside, we note that the resulting sensitivities to a_{ij} of growth GR_1 over one time step is just the proportion of the j'th stage in the initial population vector, independently of the form of A or the size of the time step, indicating the importance of the initial population vector. If the initial population vector is the SSD, the growth is λ and one might expect to obtain the sensitivities of the asymptotic growth rate λ, but the two formulae only agree if the reproductive value vector w of A equals e, which one would not expect. The difference stems from the fact that in computing the sensitivities of the asymptotic growth rate, the population vector v is the SSD and thus depends on a_{ij} too, whereas for the transient growth rate v is fixed. Moreover, if $v_j = 0$, then the transient sensitivity with respect a_{ij}, any i, is zero, because no variation in a_{ij} can effect GR_1 when v_j is zero.

We adapted Koons *et al*.'s notion of sensitivities of transient growth to our purposes by taking the partial derivatives of (S40) with respect to entries of A, which results in the following formula:

$$\frac{\partial G}{\partial a_{ij}} = \frac{\sum_k A_j^k n_k + \left(\sum_k A_k^i \right) n_j}{e' n}, \qquad \text{(S33)}$$

where here A_j^k denotes the entry of the matrix A in the j'th row and k'th column and n_k denotes the k'th component of n. These sensitivities indicate the dependence on the matrix entries of the transient one-year growth projections from actual SKKR states, which might warn the manager of unusual transient demographics. We converted sensitivities to elasticities in the usual manner (Caswell 2001:226). Note that our GR in (S31) is homogeneous of degree two in the entries of A, so by Euler's formula (Caswell 2001:229), our elasticities will sum to two.

For most nonzero entries of A, the sensitivities varied without obvious pattern across the years, except that, for both sexes, those for subadult fecundity (F_S and M_S) and the transition probabilities from S to A ($G_{\mathrm{FS3}\to\mathrm{FA}}$ and $G_{\mathrm{MS3}\to\mathrm{MA}}$) tended to decrease, while those for female adult fecundity (F_A and M_A) and adult survival (P_{FA} and P_{MA}) tended to increase, as one might expect for a long-lived species. The same patterns were observed for the elasticities.

Table S7 Means ± SD for the sensitivities and elasticities of GR (S31) computed by (S33) and sensitivities and elasticities of the dominant eigenvalue of MM1.

Matrix entry	Sensitivity of λ	Mean (sensitivity of GR) ± SD	Elasticity of λ	Mean (elasticity of GR) ± SD
F_S fecundity	0.070	0.178 ± 0.117	0.0059	0.0142 ± 0.0086
F_A fecundity	0.315	0.558 ± 0.067	0.0307	0.0515 ± 0.0062
FC1a → FC1b	0.039	0.062 ± 0.019	0.0366	0.0552 ± 0.0169
FC1b → FC2	0.039	0.057 ± 0.028	0.0366	0.0512 ± 0.0247
FC2 → FC2	0.091	0.157 ± 0.040	0.0542	0.0888 ± 0.0222
FC2 → FS1a	0.105	0.156 ± 0.040	0.0366	0.0515 ± 0.0129
FS1a → FS1b	0.039	0.052 ± 0.018	0.0366	0.0460 ± 0.0160
FS1b → FS2a	0.039	0.043 ± 0.029	0.0366	0.0386 ± 0.0259
FS2a → FS2b	0.039	0.042 ± 0.022	0.0366	0.0369 ± 0.0199
FS2b → FS3	0.039	0.051 ± 0.039	0.0366	0.0453 ± 0.0344
FS3 → FS3	0.119	0.191 ± 0.116	0.0825	0.1249 ± 0.0344
FS3 → FA	0.127	0.194 ± 0.118	0.0307	0.0444 ± 0.0268
FA → FA	0.570	0.606 ± 0.074	0.5396	0.5436 ± 0.0671
M_S fecundity	0	0.178 ± 0.108	0	0.0111 ± 0.0067
M_A fecundity	0	0.558 ± 0.067	0	0.0399 ± 0.0048
MC1a → MC1b	0	0.054 ± 0.019	0	0.0485 ± 0.0172
MC1b → MC2	0	0.049 ± 0.038	0	0.0438 ± 0.0342
MC2 → MC2	0	0.116 ± 0.050	0	0.0672 ± 0.0291
MC2 → MS1a	0	0.115 ± 0.049	0	0.0362 ± 0.0156
MS1a → MS1b	0	0.036 ± 0.014	0	0.0317 ± 0.0124
MS1b → MS2a	0	0.029 ± 0.023	0	0.0254 ± 0.0201
MS2a → MS2b	0	0.027 ± 0.015	0	0.0239 ± 0.0137
MS2b → MS3	0	0.033 ± 0.029	0	0.0295 ± 0.0260
MS3 → MS3	0	0.190 ± 0.094	0	0.1411 ± 0.0688
MS3 → MA	0	0.191 ± 0.094	0	0.0271 ± 0.0132
MA → MA	0	0.317 ± 0.068	0	0.2827 ± 0.0609

One can think of a given annual projection of an SKKR population vector and the corresponding *GR* as the growth expected over the next year. Any unusual departure in the rankings of sensitivities and elasticities of *GR* to the matrix entries of the female component of the matrix model to those of λ could serve as a warning of unusual transient dynamics, which might be relevant to management practices. In the present case, there do not appear to be any warning bells of very unusual demography. The patterns in sensitivities and elasticities were similar for both transient and asymptotic growth rates.

In summary, the matrix model projections converged towards the SSD over the modelled period 1998–2008, indicating the dynamics were mildly transient during this period in the sense that the projections were not already in the SSD. Moreover, the projected annual growth rates (S31) each year 1998–2007 differed by less than 1.8% from the asymptotic growth rate λ (Table S6). The transient sensitivities and elasticities (Table S7) did not indicate any surprising departures from expectations based on asymptotic dynamics.

Demographic Stochasticity of the Structured Population Dynamics

Sæther *et al*. (1998b) used a complicated procedure (some details of which were unpublished) to estimate demographic and environmental stochasticity for brown bears accounting for their population structure. Engen *et al*. (2005) developed a simpler method based on matrix models and obtained, for long-lived vertebrates that produce only a single offspring per breeding occasion, and assuming no relationship between reproduction and subsequent adult survival and no environmental stochasticity, an equation that estimates demographic stochasticity from the deterministic (female-only) matrix model presumed to underlie the dynamics. It appears plausible to apply this equation to the female segment of our matrix model. Engen *et al*.'s equation (13) is written down for an age-structured population but it is a simple matter to extend it to a stage-based matrix model. Recall that λ is the same for the full and female-only matrix models. Let (u_i) be the SSD of a female-only matrix model and let (v_i) be the reproductive value vector, normalized to have unit scalar product with the SSD. Then,

$$\sigma_d^2 = \frac{1}{\lambda^2} \sum_{i,j} (v_i)^2 u_j a_{ij} (1 - a_{ij}) \qquad \text{(S34)}$$

where the summation is over nonzero entries of the projection matrix $A = (a_{ij})$. The value obtained for matrix model MM1 was 0.105 (0.106 for MM2), which is for a mi-annual time step. For annual time steps, we applied (S34) to $Z = A^2$, which is the projection over one year, obtaining 0.204 for MM1.

References

Bates, D. M. & Watts, D. G. 1988 *Nonlinear Regression Analysis and Its Applications*. Hoboken: Wiley.

Doncaster, C. P. 2008 Non-linear density dependence in time series is not evidence of non-logistic growth. *Theoretical Population Biology* **73**, 483–489.

Engen, S. Bakke, Ø. & Islam, A. 1998 Demographic and environmental stochasticity-Concepts and definitions. *Biometrics* **54**, 840–846.

Fox, G. A. & B. E. Kendall 2002 Demographic stochasticity and the variance reduction effect. *Ecology* **83**, 1928–1934.

Kendall, B. E. & Fox, G. A. 2002 Unstructured individual variation and demographic stochasticity. *Conservation Biology* **17**, 1170–1172.

Melbourne, B. A. and Hastings, A. 2008 Extinction risk depends strongly on factors contributing to stochasticity. *Nature* **454**, 100–103.

Owen-Smith, N. 1990 Demography of a large herbivore; the Greater kudu *Tragelaphus strepsiceros*, in relation to rainfall. *Journal of Animal Ecology* **59**, 893–913.

Sæther, B.-E. & Engen, S. 2002 Including uncertainties in population viability analysis using population prediction intervals. In: *Population Viability Analysis*, S. R. Beissinger and D. R. McCullough (eds.), Chicago University Press, Chicago, 191–212.

Sibly, R. M., Barker, D., Denham, M. C., Hone, J. & Pagel, M. 2005 On the Regulation of Populations of Mammals, Birds, Fish, and Insects. *Science* **309**, 607–610.